

## ***Kinetic Analysis of BCL11B Multisite Phosphorylation–Dephosphorylation and Coupled Sumoylation in Primary Thymocytes by Multiple Reaction Monitoring Mass Spectroscopy***

The Faculty of Oregon State University has made this article openly available.  
Please share how this access benefits you. Your story matters.

<b>Citation</b>	Vogel, W. K., Gafken, P. R., Leid, M., & Filtz, T. M. (2014). Kinetic Analysis of BCL11B Multisite Phosphorylation–Dephosphorylation and Coupled Sumoylation in Primary Thymocytes by Multiple Reaction Monitoring Mass Spectroscopy. <i>Journal of Proteome Research</i> , 13(12), 5860-5868. doi:10.1021/pr5007697
<b>DOI</b>	10.1021/pr5007697
<b>Publisher</b>	American Chemical Society
<b>Version</b>	Accepted Manuscript
<b>Terms of Use</b>	<a href="http://cdss.library.oregonstate.edu/sa-termsfuse">http://cdss.library.oregonstate.edu/sa-termsfuse</a>

# Kinetic Analysis of BCL11B Multisite Phosphorylation– Dephosphorylation and Coupled Sumoylation in Primary Thymocytes by Multiple Reaction Monitoring Mass Spectroscopy

*Walter K. Vogel,<sup>1</sup> Philip R. Gafken,<sup>2</sup> Mark Leid,<sup>1,3</sup> Theresa M. Filtz<sup>1\*</sup>*

<sup>1</sup> Department of Pharmaceutical Sciences, College of Pharmacy, Oregon State University, Corvallis,  
Oregon 97331, United States

<sup>2</sup> Fred Hutchinson Cancer Research Center, 1100 Fairview Avenue North, Seattle, Washington 98109,  
United States

<sup>3</sup> Integrative Biosciences Department, School of Dentistry, Oregon Health & Science University, 611  
SW Campus Drive, Portland, Oregon 97239-3097 United States

**Keywords:** BCL11B, MRM, Post-translational modification, Signal transduction, SRM, Sumoylation,  
T-cell receptor

## **ABSTRACT**

Transcription factors with multiple post-translational modifications (PTMs) are not uncommon, but comprehensive information on site-specific dynamics and interdependence is comparatively rare. Assessing dynamic changes in the extent of PTMs has the potential to link multiple sites both to each other and to biological effects observable on the same time scale. The transcription factor and tumor suppressor BCL11B is critical to three checkpoints in T-cell development and is a target of a T-cell receptor (TCR)-mediated MAP kinase signaling. Multiple reaction monitoring (MRM) mass spectroscopy was used to assess changes in relative phosphorylation on 18 of 23 serine and threonine residues and sumoylation on one of two lysine residues in BCL11B. We have resolved the composite phosphorylation–dephosphorylation and sumoylation changes of BCL11B in response to MAP kinase activation into a complex pattern of site-specific PTM changes in primary mouse thymocytes. The site-specific resolution afforded by MRM analyses revealed four kinetic patterns of phosphorylation and one of sumoylation, including both rapid simultaneous site-specific increases and decreases at putative MAP kinase proline-directed phosphorylation sites, following stimulation. These data additionally revealed a novel spatiotemporal bisphosphorylation motif consisting of two kinetically divergent proline-directed phosphorylation sites spaced five residues apart.

## **INTRODUCTION**

PTMs are the key regulatory handles responsible for altering the functional state of cellular proteins. Individually, in multiples, or in combinations they can alter secondary structure, enzymatic activity, protein–protein and protein–complex interactions, subcellular localization, and thermodynamic or

regulated stability. These finely coordinated modifications are critical to proper cell function; miscoordination of these PTMs, including PTMs of transcription factors,<sup>1</sup> is associated with aberrant cell function and disease.<sup>2-4</sup>

Site-specific DNA-binding transcription factors directly regulate gene expression to control everything from the very nature of a cell—coordinating development through functional maturity—to finely tuned and subtle responses to internal and external cues. Having no constitutive enzymatic activities, transcription factors are the orchestrating nucleus for associating enzymatic complexes and are themselves the target and integrator of cellular signals in the form of PTMs.<sup>1</sup> The site-specific transcription factor BCL11B is required for postnatal life and proper development of skin,<sup>5</sup> teeth,<sup>6,7</sup> and the nervous system.<sup>8,9</sup> BCL11B is essential to the development and function of the adaptive immune response and is highly expressed in the T-cell lineage. Circulating T-cell subtypes develop in the thymus, where BCL11B serves as a master regulator and determining transcription factor for T-cell lineage commitment.<sup>10-15</sup> The latter stages of thymocyte development are regulated by activation of the T-cell receptor (TCR) and downstream MAP kinase pathways, which in turn activate a gene network sufficient for the T cell maturation program (positive selection) or for induction of apoptosis (negative selection). Knockout of BCL11B blocks T-cell development.<sup>12,15</sup> In late-maturing double-positive (DP) thymocytes, BCL11B regulates expression of approximately 900 genes, functioning as a repressor in the context of the NuRD complex of proteins at a majority of the sites but functioning as an activator at a minority (33%).<sup>14</sup> In humans, haploinsufficiency of BCL11B is linked to T-cell acute lymphoblastic leukemia<sup>16-18</sup> and adult T-cell leukemia/lymphoma;<sup>19</sup> BCL11B over-expression is associated with acute myeloid leukemia<sup>20</sup> and head and neck squamous cell carcinoma.<sup>21</sup> In mice, haploinsufficiency of BCL11B increases susceptibility to radiation-induced lymphomas and lymphoblast crisis.<sup>22</sup>

BCL11B is a highly phosphorylated transcription factor with more than 50 sites in human and 37 in mouse tissues reported to date.<sup>23</sup> In mouse primary thymocytes, we previously identified 23 serine/threonine phosphorylation sites and two sites of sumoylation of BCL11B.<sup>24</sup> Our study showed that BCL11B is modified by phosphorylation and sumoylation in resting thymocytes (90% of which are DP cells) and responds dynamically to activation of the MAP kinase signaling pathway. Activation leads to the following composite changes in BCL11B: 1) a rapid increase in phosphorylation and coincident loss of basal sumoylation that is 2) followed by simultaneous dephosphorylation and resumoylation, and 3) subsequent ubiquitination and proteasomal degradation. BCL11B phosphorylation is mediated by both ERK1/2 and p38 MAP kinases but the slower dephosphorylation is dependent on ERK1/2-activated protein phosphatases. The sumoylation state of BCL11B is dependent on the activity of associated SENP desumoylating enzymes and this activity is promoted by BCL11B phosphorylation. The consequence of these sequential PTM changes is the apparent conversion of BCL11B from a repressor to an activator of transcription at the model target gene, *Id2*.

The role(s) of BCL11B PTMs is underexplored in normal thymocyte function as are the consequences of its dysregulation in oncogenesis. Tandem mass spectrometry was used to directly identify the principal sumoylation site (for both SUMO1 and SUMO2/3).<sup>24</sup> However, despite identifying a linkage between phosphorylation and desumoylation, we lacked phosphorylation site-specific kinetic information needed to efficiently interrogate functional effects of BCL11B PTMs efficiently. To define the functionally relevant phosphosite alterations that precede or complement sumoylation to regulate BCL11B activity, resolution of the kinetics of phosphorylation/dephosphorylation of individual phosphosites—including those occurring on multiply-phosphorylated peptides—is required over a time course of activation corresponding to changes in transcriptional activity.

The current report is focused on resolving the dynamics of phosphorylation and sumoylation on BCL11B in a native cell system, i.e. thymocytes, with naturally-limited protein levels using multiple reaction monitoring-mass spectrometry (MRM-MS). Detailed kinetic characterization has the potential to distinguish the most relevant PTMs of highly modified proteins, and narrow the combinatorial scope of lower throughput methods that seek to define the function of identified PTMs. We characterized the relative PTM dynamics of the majority of BCL11B phosphosites and its principal sumoylation site and grouped these sites into kinetically-concerted sub-populations.

## **MATERIALS AND METHODS**

### **Primary Cell Culture and Treatment**

Primary mouse thymocytes were isolated from 5–7 week old mice and cultured at 37 °C in RPMI 1640 media supplemented with 2.5% fetal bovine serum (HyClone) for 6 h prior to chemical stimulation. All procedures involving mice were conducted with approval of the Oregon State University Institutional Animal Care and Use Committee. Thymocytes were stimulated with 100 nM phorbol 12,13-dibutyrate (LC Labs, Woburn, MA) and 500 nM A23187 (Calbiochem), or with DMSO (vehicle control), for between 7 and 60 min to activate cell signaling pathways in a manner similar to native T-cell activation.<sup>25,26</sup>

### **Protein Extraction and Sample Preparation**

Immediately after treatment, cultured thymocytes were diluted in ice-cold PBS, centrifuged, and lysed in 10 volumes of rapid detergent lysis buffer (20 mM HEPES pH 7.4, 200 mM NaCl, 50 mM NaF, 2 mM EDTA, 10% glycerol, 0.1 mM PMSF, 1  $\mu$ g/ml pepstatin A, 5  $\mu$ g/ml leupeptin, 10  $\mu$ M E64, 10 mM *N*-ethylmaleimide, and 1% SDS) and placed in a boiling water bath for 15 min. Denatured protein

extracts were sonicated to shear DNA and diluted ten-fold in the same buffer lacking SDS but containing 1.1% Triton-X100. Two monoclonal anti-BCL11B antibodies (clones 25B6, Abcam ab18465 and 6A10, mAbDx, Cambridge, MA) were used together, each at 0.25  $\mu\text{g/mL}$ , to immunoprecipitate denatured BCL11B from dilute extracts. BCL11B samples were gel purified from protein G agarose immune complexes by SDS-PAGE and peptides prepared for analysis by sequential cyanogen bromide cleavage and trypsin digestion. In-gel cyanogen bromide digests (200 mM cyanogen bromide in 70% trifluoroacetic acid) were conducted at room temperature for 12–14 h, protected from light in a fume hood. Warning: cyanogen bromide is toxic, volatile, and decomposes to HCN gas. Volatile reactants were removed from the gel slices by centrifugal vacuum concentration, neutralized with ammonium bicarbonate, and dehydrated in acetonitrile. Prior to tryptic digestion, the dried gel slices were rehydrated and reduced in 25 mM dithiothreitol/50 mM ammonium bicarbonate for 30 min at 50 °C, alkylated in 50 mM 2-chloroacetamide/50 mM ammonium bicarbonate for 30 min at room temperature, and dehydrated again in acetonitrile. In-gel tryptic digests were conducted in 0.025% ProteaseMax (Promega, Madison, WI), 50 mM ammonium bicarbonate for 3 h at 37 °C. Product peptides were extracted from gel slices in 0.01% ProteaseMax, 50 mM ammonium bicarbonate, acidified with trifluoroacetic acid, and concentrated by vacuum centrifugation. This double-cleavage procedure permitted the efficient analysis of phosphorylation on Ser169, Ser277, Ser401, and Thr416, and sumoylation on Lys679. The signals from the resulting shorter peptides were more easily observed and the site-specific resolution of phospho-Ser401 from phospho-Thr416 was facilitated by analyzing these modifications on separate peptides generated from the cleavage at Met412. Cyanogen bromide cleavage also facilitated the analysis of sumoylation by reducing the size of the SUMO moieties from between 19 residues (SUMO1) and 34 residues (SUMO2 and SUMO3) to 15 residues. The cleavage products of

SUMO2 and SUMO3 are indistinguishable; consequently, we are reporting the combined modification by both of these subtypes (see Supplemental Figures 1 and 2 for outlines of sample preparation).

### **Targeted Mass Spectrometry Analysis**

Sample solutions were analyzed on a Thermo TSQ Vantage triple quadrupole mass spectrometer (Thermo-Fisher Scientific, Waltham, MA) in the MRM mode. The mass spectrometer used the Xcalibur control software (version 2.1) with Thermo EZ-Tune (version 2.3 SP1) and was coupled to an Eksigent NanoLC 2-dimensional HPLC system (Dublin, CA) with a Peltier cooled (model AS-1) autosampler. A 10  $\mu$ L sample was loaded onto a 2 cm  $\times$  100  $\mu$ m inner diameter IntegraFrit trap column (New Objective, Woburn, MA) packed with Magic C<sub>18</sub> 200 Å pore size, 5  $\mu$ m diameter reverse-phase resin (Michrom Bioresources, Auburn, CA) and eluted from a 21 cm  $\times$  75  $\mu$ m inner diameter PicoFrit capillary column (New Objective) packed with Magic C<sub>18</sub> reverse-phase resin (100 Å, 5  $\mu$ m) using a 45-min gradient from 2% to 40% solvent B in solvent A, followed by a 5 min gradient to 60% solvent B, and then a 1 min gradient to 95% solvent B at a flow rate of 400 nL/min, where solvent A was 0.1% formic acid in water and solvent B was 0.1% formic acid in acetonitrile. The solvents used were LC-MS grade from Burdick & Jackson (Morristown, NJ). Spectra were acquired over a 75 min period using a resolution of 0.7 (fwhm) in both Q1 and Q3, a chrom filter peak width of 10 s, and a collision gas pressure on Q2 of 1.2 mTorr. The spray voltage used was set at a value to establish a stable spray, which ranged between 1850–2100 V, and the capillary temperature was set to 275 °C.

### **Quantitative Multiple Reaction Monitoring Analysis**

Analytical precursor/product ion pair transitions were chosen from a spectral library generated using BiblioSpec (version 2)<sup>27</sup> from Thermo LTQ-FT tandem mass data<sup>24</sup> and optimized on a TSQ Vantage triple quadrupole mass spectrometer with respect to collision energy.<sup>28</sup> Skyline (version 1.3)<sup>29</sup> MRM



analysis software was used to generate a series of collisional energy (CE) optimization methods for the mass spectrometer. Unscheduled transition lists were exported into fifteen MRM-mode instrument methods to allow higher scan time (15 ms) analysis of transitions. For each transition, a range of collisional energy voltages spanning  $\pm 5$  volts from a theoretically calculated optimal value were recorded and these qualification runs were evaluated in Skyline. The CE voltage which yielded the highest intensity peak for each peptide was determined to be the optimal value (see Supplemental Figure 3 for transitions to spectra library matches used in this study). The scan time used in the finalized transition list was 8 ms.

Relative quantitative analysis was based on the sum of precursor/product ion pair total ion currents of PTM-containing peptides normalized to total BCL11B represented by unmodified BCL11B peptides. Analytical transitions were recorded for each peptide and site-specific transitions were chosen to resolve phosphorylations on multiply phosphorylated peptides. See Figure 1 for an outline of analytical procedures and Supplemental Table 1 for a listing of transitions used in these analyses. Our choices for normalization peptides in this highly modified protein were limited as many of the best candidates contained known or potential phosphorylation sites. We used a pair of BCL11B tryptic peptides lacking known or potential phosphorylation sites,  $^{437}\text{FQSNLIVHR}^{445}$  and  $^{641}\text{GGAFAPGAEPFPALFPR}^{657}$ , for signal normalization in most instances (the signals used to quantify these peptides are shown in Supplemental Figure 4). An alternative normalization procedure used the non-phosphorylated version of analyzed peptides, where possible, for the peptide products of cyanogen bromide cleavage as the efficiency of this reaction was variable. Cyanogen bromide will not cleave oxidized methionine residues,<sup>30</sup> and the source of this variability was likely sample differences in the degree of methionine oxidation. Using these non-phosphorylated peptides for normalization was an effective internal sample control. Phosphorylation at Thr376 and Ser381 were quantified as the unweighted mean of the

normalized signals from two peptides; all other sites were quantified from a single peptide. Data from two independent biological replicate samples are reported.

### **Data Access**

The mass spectrometry data have been deposited to PeptideAtlas database (PASSEL, <http://www.PeptideAtlas.org>)<sup>31</sup> with the dataset identifier PASS00521. Quantitative chromatograms and the spectral library are available for viewing at [https://panoramaweb.org/labkey/project/OSU\\_Filtz\\_Group/supplementary\\_data/Vogel-2014/begin.view?](https://panoramaweb.org/labkey/project/OSU_Filtz_Group/supplementary_data/Vogel-2014/begin.view?) and are available from the same location for download as Skyline files (Skyline software<sup>29</sup> is freely available at <https://skyline.gs.washington.edu>).

## **RESULTS AND DISCUSSION**

The kinetics of phosphorylation of individual sites in multiply phosphorylated proteins is greatly understudied, and yet is critical for accurately determining the mechanistic role of post-translational modifications in regulation of protein function. Most PTMs are viewed as binary switches in which presence or absence controls a discreet protein function or location. In multiply modified proteins, the potential tertiary structures or modification states increase as do the opportunities for fine-tuning response or for variation in function. Currently, mass spectrometric techniques used to identify PTMs are far more efficient than methods available to assess the functional relevance of the modifications. Two strategies are generally used to identify functional effects of PTMs. The first strategy is to develop site-specific antibodies selective for modified states of the protein, and probe under various conditions to correlate modification with function. This method is robust and applicable to native tissues; however, developing and validating antibodies requires a significant investment of time and resources and is impractical as a survey method. The second strategy is mutagenesis of the modified site to a non-

modifiable amino acid and/or mutagenesis to a mimic (e.g. mutation to glutamate to mimic a phosphosite) followed by assessment of function. However, studying highly modified proteins by mutagenesis of individual sites presents significant difficulty in that combinatorial possibilities can overwhelm experimental designs. Although a few reports exist in which clusters of relevant PTMs were identified by simultaneous multi-site mutants (e.g., the roles of combinations of 26 phosphosites in the plant transcription factor PIF3<sup>32</sup>), we have had only limited success in identifying the function of specific phosphorylation sites after creating numerous single and multi-phosphosite mutants of BCL11B.<sup>24</sup> To more efficiently identify functional clusters of PTMs on BCL11B, we hypothesized that functional states of the protein are likely to temporally correlate to the PTM kinetics of individual sites. To most accurately link PTMs to temporally distinct functions, we sought to quantify the kinetics of modification of individual amino acid residues over the functional time course in the native system, DP thymocytes.

Given these constraints, we selected MRM-MS to attempt comprehensive quantification of relative modifications of all identified sites of BCL11B over a time course of activation. A recent study by Zheng and colleagues<sup>33</sup> used MRM-MS analysis to link five phosphosites in the scaffolding protein SHC1 to at least three distinct phosphorylation states that temporally correlated with segregated functional outcomes following EGF receptor stimulation. The challenge that we faced was to perform a similar MRM-MS analysis but in a native tissue source with its normal repertoire of PTM modifying enzymes at naturally limited protein levels, simultaneously quantifying 23 previously-identified phosphorylation sites.

BCL11B PTMs were assessed by MRM-MS basally and at three time points based on previous estimates of the maxima of each PTM following the initiation of MAP kinase stimulation by PDBu/A23187 to quantify site-specific dynamics in primary mouse thymocytes.<sup>24</sup> The stimulation time

points also encompass the timeframe in which BCL11B functionally shifts from association with a repressed to an activated *Id2* target gene. Sample PTMs were preserved by rapid whole cell denaturation; the target protein was enriched by immunoprecipitation and gel purified prior to analysis. Analytical transitions were chosen to quantify PTM-containing peptides and site-specific transitions were chosen for multiply phosphorylated peptides. The method effectively resolved the site-specific phosphokinetics of multiply phosphorylated peptides and allowed us to quantify 18 of 23 phosphorylation sites. Our results are consistent with a more limited previous report that BCL11B is dynamically phosphorylated at four specific sites in TCR-stimulated human leukemia T (Jurkat) cells.<sup>34</sup> For the analysis of BCL11B sumoylation, fragment ions encompassing the entire tryptic pentapeptide and between 2 and 11 residues of the SUMO moieties were chosen. Relative PTM quantification efficiently served the primary purpose of identifying amplitude and kinetics of dynamically modified residues. Absolute quantification can be accomplished by the use of stable isotope-labeled internal standard peptides,<sup>35,36</sup> but given 23 sites to monitor this would have been needlessly costly for our purposes.

MRM analysis is commonly used to quantify proteins from complex mixtures in proteomic studies by identifying a few experimentally well-behaved peptides and selectively monitoring a few of the most intense collisionally-induced precursor/product ion pairs. However, the single-protein, multisite analyses performed herein did not allow the freedom to choose the most intense peptides. Therefore, the signals obtained and quantified in this study are generally smaller than those expected for a proteomic study. The low stoichiometric ratio typical of many PTMs imposes an additional analytical limitation. Despite increasing sample size, data for five additional phosphorylation sites previously identified<sup>24</sup> were not sufficiently robust to permit site-specific quantification.

## Sumoylation Is More Easily Assessed with Cyanide Bromide Cleavage

BCL11B has two known sumoylation sites: the principal site, Lys679, was identified *in situ* by tandem mass spectrometry; and a secondary site, Lys877, which is not amenable to mass spectrometry analysis, was identified from the results of site-directed mutagenesis.<sup>24</sup> Our analysis of BCL11B sumoylation was limited to the modification of the experimentally accessible Lys679 by SUMO1 and SUMO2/3 and was aided by the combined use of cyanogen bromide cleavage and trypsin digestion, which provided a significant advantage over trypsin alone for the analysis of sumoylation. Cyanogen bromide cleaves the SUMO side chains to 15 amino acid residues for all subtypes and reduces the number of isoforms resulting from missed trypsin cleavage (relevant to the analysis of SUMO2/3). These shortened SUMO moieties retain the same sequence distinction as the trypsin-only digestion products and for most peptides are expected to be predominantly observed as 3<sup>+</sup> charge state ions when analyzed by electrospray ion sources. The signals generated by these smaller branched chain peptides proved sufficient for the current analysis. Cyanogen bromide/tryptic preparations may be generally useful for the mass spectrometric analysis of sumoylation.

The kinetics of Lys679-specific sumoylation quantified by MRM-MS are similar to the non-site specific quantitative immunoblot analysis (Supplemental Figure 5). Sumoylation decreased rapidly upon thymocyte stimulation followed by resumoylation to a level greater than basal by 60 min. Sumoylation often results in the multimeric attachment of SUMO moieties to a single lysine residue forming polymeric chains, potentially of mixed subtypes<sup>37</sup> and observed for BCL11B in this context (see Supplemental Figure 5 and REF 24). Immunological methods are sensitive to the total number of SUMO moieties but the mass spectrometric methods employed in the current report are sensitive only to the covalent attachment stoichiometry at the target lysine residue.

BCL11B may be ideally suited to the study of sumoylation dynamics in a native, functionally relevant cell population. Its principal sumoylation site is located on a small tryptic peptide five amino acids in length, placing this modification within the analytical range of current, targeted mass spectrometric techniques. In contrast, a typical sumoylated peptide analyte is expected to be the length of two typical tryptic peptides modified by the addition of a 15 amino acid SUMO moiety. In addition, BCL11B is natively expressed at high levels in thymocytes; a cell population that is highly homogeneous and easily isolated from the thymus. Finally, the dynamics of BCL11B PTMs are easily and relevantly affected as demonstrated in the current report.

### **Kinetic Classification of BCL11B Post-translational Modifications**

Kinetic characterization of the phosphorylation sites revealed that the composite phosphorylation status of BCL11B previously observed over the stimulation time course was not the result of simultaneous, kinetically concerted alterations of all sites. Rather, resolution of the sumoylation and phosphorylation kinetics of individual sites allowed us to classify distinct PTM states of BCL11B. Phosphosites were categorized into four groups based on relative changes in the stoichiometry of phosphorylation. Phosphorylation of four sites increased rapidly reaching a maximum at 7 min post stimulation and decreased from there (shown in red in Figure 2). A second group of five sites (shown in green in Figure 2) lost phosphorylation relative to basal, reaching a minimum at either 7 or 30 min. For a third group of four sites (shown in blue), stimulation resulted in a general increase in phospho-stoichiometry that was relatively insensitive to phosphatase activity when compared to the red sites. The fourth group of three sites appeared to be relatively insensitive to stimulation (shown in black in Figure 2).

A summary model of these data reveals that MAP kinase stimulation elicits four successive states evident in the changing PTM pattern of BCL11B (Figure 3). The model is partially informed by

estimates of the extent of phosphorylation derived from relative phosphorylation changes (Figure 2) and comparable differences between the phosphopeptides and non-phospho-modified versions of those peptides. The basal state of the protein is sumoylated on Lys679 and phosphorylated on selected residues (green bars in Figure 3). MAP kinase stimulation simultaneously results in rapid selective dephosphorylation of some basally phosphorylated residues and increased phosphorylation at other sites. Some of the increased phosphorylation sites are relatively sensitive to phosphatase(s) and rapidly dephosphorylate (red bars) while others are not (blue bars). Stimulation also results in an initial rapid decrease in sumoylation at Lys679. Thirty minutes after the onset of stimulation, phosphorylation has reached an overall minimum and sumoylation levels have returned to near basal. By 60 min post-stimulation, the phosphorylation status of BCL11B is dominated by the kinase sensitive/phosphatase insensitive sites (blue bars) and the sumoylation state is markedly in excess of basal. The most dynamically altered amino acids fall within range of the central BCL11B protein–protein interaction domain (*PPID 1*, Figure 3).<sup>38-41</sup>

### **Desumoylation and Resumoylation Occur in Different Phospho-BCL11B Contexts**

The integration of extracellular signals and resulting changes in gene expression patterns are mediated by changes in PTM status of transcription factors and associated cofactors.<sup>1</sup> DP thymocytes are a quiescent cell type; poised for both activation and apoptosis, they are the progenitor of numerous circulating T-cell subtypes and serve as a developmental checkpoint. BCL11B is essential as its regulated activation is critical to the adaptive immune response. In the basal state, the transcription factor BCL11B is the repressor of some genes and the activator of others.<sup>14</sup> Upon cellular activation, BCL11B appears to switch from a basal repressor to a net activator of at least some of these genes via a process that involves both desumoylation and resumoylation linked to changes in phosphorylation.<sup>24</sup> While there are multiple phosphorylation site changes, these assume three distinct states in thymocytes

in response to stimulation. Basal sumoylation exists in one of these states, the rapid desumoylation occurs while BCL11B assumes a second phosphorylation state, and the subsequent resumoylation occurs while BCL11B is in a third state. Previous work had suggested no more than a simple inverse relationship between sumoylation and phosphorylation. The current report clearly indicates that resumoylation, returning to near basal levels by about 30 min and increasing to a maximum at about 60 min, occurs in the context of a phosphorylation state that is very different from that which exists under basal conditions (Figure 3). The results of this analysis suggest that a particular combination of phosphorylation sites in the presence of sumoylation is needed to specify the activity state of BCL11B-occupied promoters.

### **Identification of a Novel Spatiotemporal Bisphosphorylation Motif**

The kinetic resolution obtained in these studies also allowed for identification of two instances of a previously unidentified spatiotemporal protein phosphorylation motif, pTPPXXpSP, in BCL11B, the subsites of which share a similar kinetic and directional response to MAP kinase stimulation. Shown in Figure 2 and schematically in Figure 3, both threonines (Thr313 and Thr376) are relatively phosphorylated in the basal state while the serines (Ser318 and Ser381) are relatively unphosphorylated. Upon MAP kinase stimulation, the threonines are rapidly dephosphorylated while the serines phosphorylated, suggesting differential sensitivity of the sites to kinase and phosphatase. The effect of cellular stimulation is to switch the dominant phosphosite on both motifs from the threonine to the serine residues.

The closest analogous example of this motif occurs in the transcription factor MYC. This extensively studied protein is activated and degraded by sequential phosphorylation–dephosphorylation on a closely spaced pair of proline-directed phosphorylation sites. MYC is sequentially phosphorylated first at Ser62 and then at Thr58 by different kinases, the first of which activates and stabilizes the protein while the

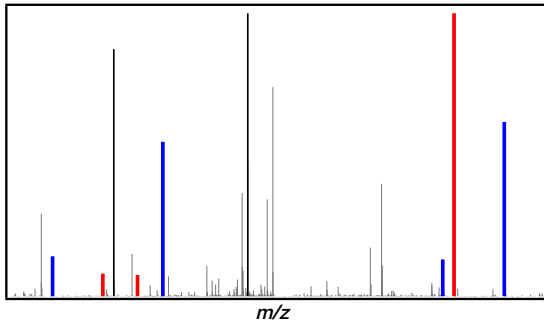


second is required for the binding of PIN1, the consequent *cis/trans*-isomerization of Pro63, and the degradation promoting dephosphorylation of phospho-Ser62 by a *trans*-specific phosphatase. These motifs while similar at the amino acid sequence level differ in the sequential ordering of phosphorylation and dephosphorylation and in the consequence of dephosphorylation.<sup>3,42</sup>

This BCL11B motif is relatively uncommon, occurring singly in approximately 60 human proteins, half of which are known to be phosphorylated (see Supplemental Table 3) and three of which have known functional relevance, including in the cardiac hypertrophic response mediated by the transcription factor GATA4.<sup>2,43,44</sup> BCL11B uniquely contains two examples of the motif both occurring in the middle of the central protein–protein interaction domain (Figure 3). While the microscopic mechanism underlying the switch in the motif is likely rooted in the differential sensitivity to signal-activated protein phosphatases, the macroscopic effect may be as a signal coincidence detector for the dual activation of both relevant kinases and phosphatases.

## CONCLUSION

MAP kinase activation in thymocytes results in a complex pattern of multisite phosphorylation, dephosphorylation, desumoylation, and resumoylation on the target transcription factor BCL11B. While these results are consistent with the simultaneous action of ERK- and p38-mediated phosphorylation and ERK-stimulated phosphatase action,<sup>24</sup> the resulting multiple kinetic patterns are unusual. Multisite phosphorylation/dephosphorylation is often observed to be concerted and sometimes positively cooperative, resulting in switch-like mechanisms.<sup>45–48</sup> The four kinetic patterns of phosphorylation we observe suggest a complicated PTM-mediated regulatory scheme requiring the action of multiple enzymes, the interplay of which remain to be defined. The bisphosphorylation motif described above may be an example of this complexity.

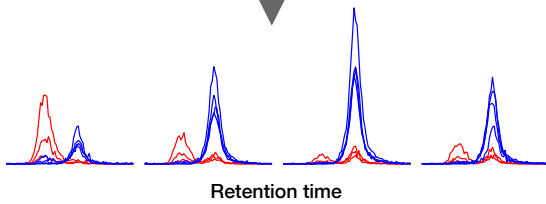


- Spectral library assisted selection of PTM site-specific transitions

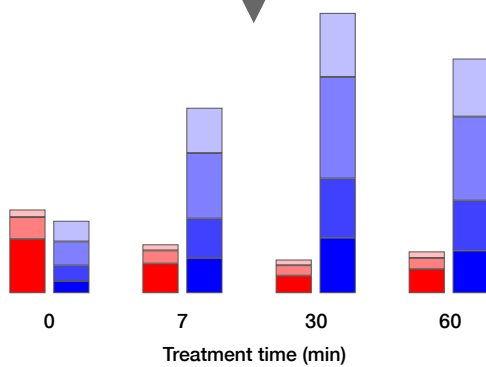


nanoLC QqQ-MS

- Transition collision energy optimization
- Data collection



- Sample signal normalization



- Quantification as the sum of integrated signal intensities

**Figure 1.** Outline of site-specific PTM quantification by LC-MRM. Phosphorylation of BCL11B peptides containing multiple sites was quantified by selecting residue-specific transitions from a spectral library and optimizing the collision energy of each transition to maximize signal intensity. The transitions, signal, and relative quantitative values for an example isobaric mixture of two singly phosphorylated peptides are colored in red and blue to indicate the residual locations of the phosphate modification and the site-specific divergent kinetics upon cell signaling pathway activation in primary thymocyte culture. The figure illustrates the quantification of Thr313 (red) and Ser318 (blue) from one biological replicate.

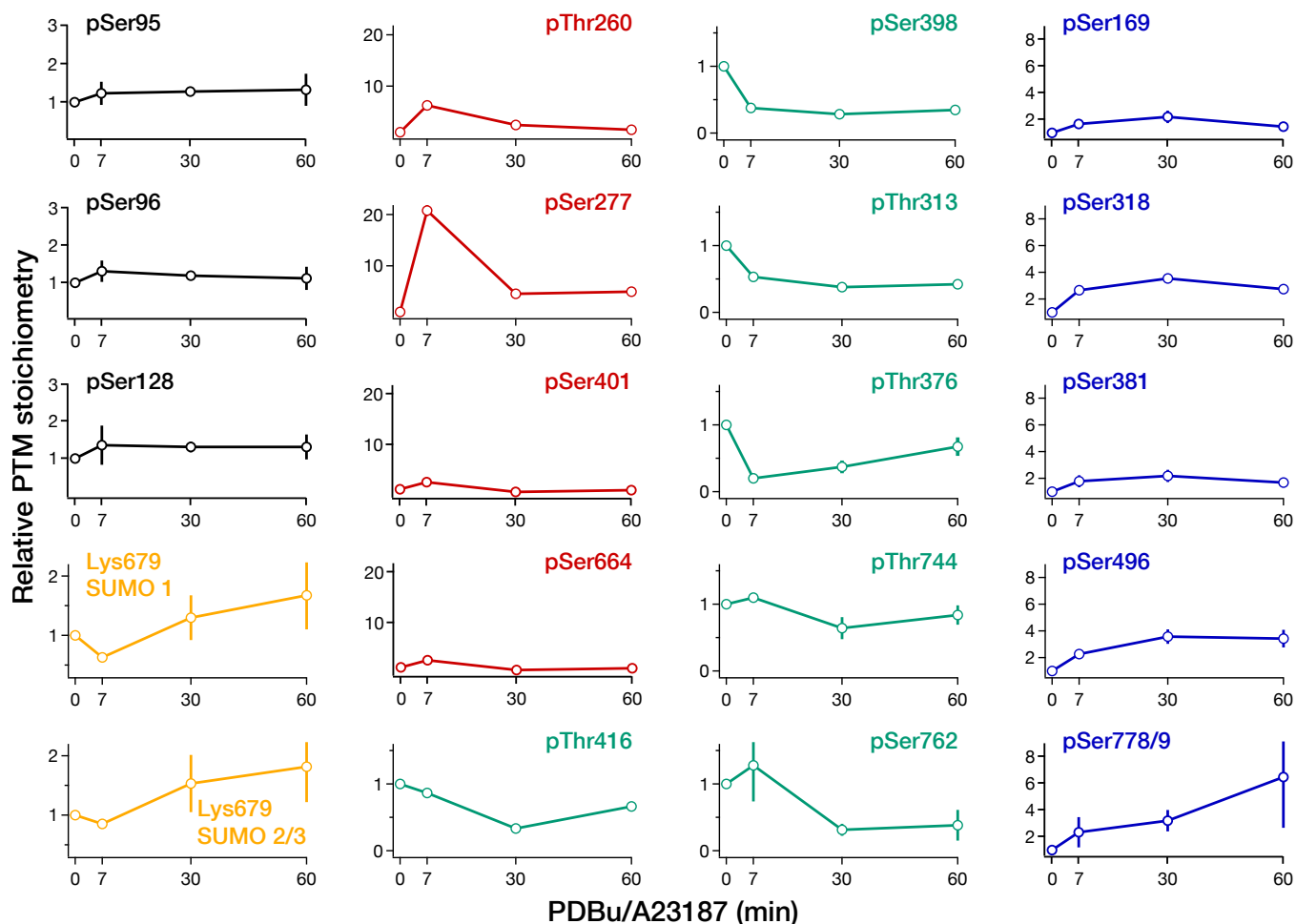


**Figure 2.** Relative quantification of BCL11B post-translational modifications following MAP kinase stimulation in primary mouse thymocytes. Site-specific quantifications were calculated from the sum of multiple total ion currents targeting PTM specific LC-MRM transitions (see Supplemental Table 1 for the specific transitions and Supplemental Table 2 for the data represented in this figure). Time of stimulation (min) is presented on the abscissa and plotted relative to basal unstimulated (0 min) on the ordinate. Specific BCL11B site modifications are identified in the figure and are grouped kinetically: sites that increase rapidly to a maximum at 7 min followed by a decrease (with a minimum at 30–60 min) are shown in red, sites that decrease from basal are shown in green, sites that increase with stimulation and remain elevated are shown in blue, sites insensitive to stimulation are shown in black, and sumoylations at Lys679 are shown in orange. Data points are the mean of two biological replicates

and the vertical bars represent the range of these data values. Data points without vertical bars did not vary beyond the width of the plotting point between the two data sets.

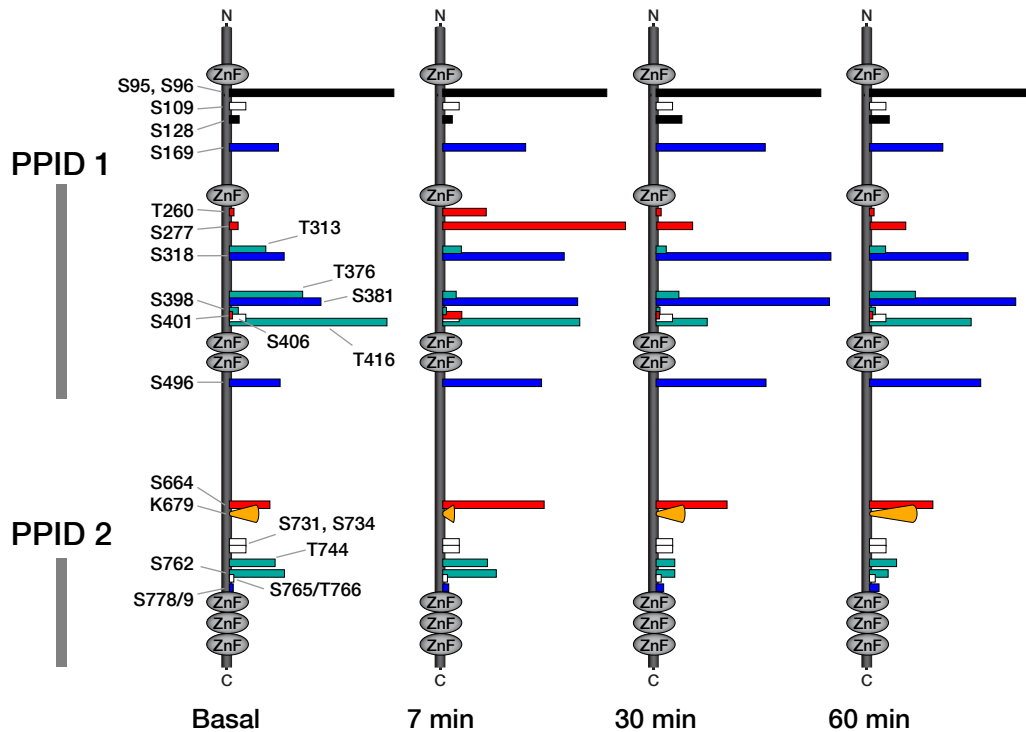


**Figure 3.** Model of BCL11B post-translational modification states. Kinetic data show that PTM status is a succession of discrete states. Bar heights indicate the relative degree of phosphorylation and sumoylation of BCL11B basally and at time points following PDBu/A23187 stimulation of primary mouse thymocytes. The bar colors are described in Figure 2 and phosphorylation sites lacking kinetic data are shown in white. The central protein–protein interaction domain for HP1 $\alpha$ ,<sup>38,40</sup> SIRT1,<sup>39</sup> CoupTF,<sup>40</sup> SP1,<sup>40</sup> and NuRD complex members RbAp46 and RbAp48<sup>41</sup> (PPID 1) and the carboxy-terminal protein–protein interaction domain for CoupTF,<sup>40</sup> HP1 $\alpha$ ,<sup>38,40</sup> and SP1,<sup>40</sup> (PPID 2) are indicated by vertical gray bars. Phosphorylation of residues Ser95 and Ser96 are combined and represented as a single bar.

## **ASSOCIATED CONTENT**

### **Supporting Information**

Supplemental Table 1. Transitions used to quantify changes in BCL11B post-translational modifications. Supplemental Table 2. Relative quantification of BCL11B post-translation modifications. Supplemental Table 3. Human Proteins with the TPPxxSP motif. Supplemental Figure 1. Outline of BCL11B sample preparation. Supplemental Figure 2. BCL11B sample preparation: gel purification. Supplemental Figure 3. Spectra database matches for analyzed peptides. Supplemental Figure 4. Relative quantification of BCL11B peptides used to normalize PTM-containing peptide signals. Supplemental Figure 5. Quantitative immunoblot analysis of BCL11B sumoylation. “This material is available free of charge via the Internet at <http://pubs.acs.org>.”

## **AUTHOR INFORMATION**

### **Corresponding Author**

\* Theresa M. Filtz, Department of Pharmaceutical Sciences, College of Pharmacy, Oregon State University, Corvallis, Oregon, 97331-3507, USA

e-mail: [Theresa.filtz@oregonstate.edu](mailto:Theresa.filtz@oregonstate.edu)

Tel.: 541-737-5802

Fax: 541-737-3999

### **Author Contributions**

The manuscript was written through contributions of all authors. All authors have given approval to the final version of the manuscript.

## **ACKNOWLEDGMENTS**

The authors wish to thank Brian Milless and Fred Hutchinson Cancer Research Center for invaluable technical support, Jeff Morrié and the Environmental Health Sciences Center Mass Spectrometry Facility at Oregon State University (supported by *NIEHS, National Institutes of Health Center Grant ES000210*) for preliminary data, and Diana Eng and Chrissa Kioussi (Oregon State University) for help with mouse husbandry. Research reported in this publication was supported by the National Institute of General Medical Science of the National Institutes of Health under award number R15 GM096243 (to T. M. F.) and by funds provided by the Oregon State University College of Pharmacy.

## **ABBREVIATIONS**

DP, double-positive thymocytes; MRM, multiple reaction monitoring; NuRD, nucleosome remodeling and deacetylation; PDBu, phorbol 12,13-dibutyrate; PTM, post-translational modification; SUMO, small ubiquitin-like modifier; TCR, T cell receptor

## **REFERENCES**

(1) Filtz, T. M.; Vogel, W. K.; Leid, M. Regulation of transcription factor activity by interconnected post-translational modifications. *Trends Pharmacol. Sci.* **2014**, *35*, 76–85.

- (2) van Berlo, J. H.; Elrod, J. W.; Aronow, B. J.; Pu, W. T.; Molkentin, J. D. Serine 105 phosphorylation of transcription factor GATA4 is necessary for stress-induced cardiac hypertrophy in vivo. *Proc. Natl. Acad. Sci. U. S. A.* **2011**, *108*, 12331–12336.
- (3) Arnold, H. K.; Sears, R. C. A tumor suppressor role for PP2A-B56 $\alpha$  through negative regulation of c-Myc and other key oncoproteins. *Cancer Metastasis Rev.* **2008**, *27*, 147–158.
- (4) Wang, Y.-C.; Peterson, S. E.; Loring, J. F. Protein post-translational modifications and regulation of pluripotency in human stem cells. *Cell Res.* **2013**.
- (5) Golonzhka, O.; Liang, X.; Messaddeq, N.; Bornert, J.-M.; Campbell, A. L.; Metzger, D.; Chambon, P.; Ganguli-Indra, G.; Leid, M.; Indra, A. K. Dual role of COUP-TF-Interacting Protein 2 in Epidermal Homeostasis and Permeability Barrier Formation. *J. Invest. Dermatol.* **2009**, *129*, 1459–1470.
- (6) Golonzhka, O.; Metzger, D.; Bornert, J.-M.; Bay, B. K.; Gross, M. K.; Kioussi, C.; Leid, M. Ctip2/Bcl11b controls ameloblast formation during mammalian odontogenesis. *Proc. Natl. Acad. Sci. U. S. A.* **2009**, *106*, 4278–4283.
- (7) Kyrylkova, K.; Kyryachenko, S.; Biehs, B.; Klein, O.; Kioussi, C.; Leid, M. BCL11B Regulates Epithelial Proliferation and Asymmetric Development of the Mouse Mandibular Incisor. *PLoS ONE* **2012**, *7*, e37670.
- (8) Arlotta, P.; Molyneaux, B. J.; Jabaudon, D.; Yoshida, Y.; Macklis, J. D. Ctip2 Controls the Differentiation of Medium Spiny Neurons and the Establishment of the Cellular Architecture of the Striatum. *J. Neurosci.* **2008**, *28*, 622–632.



- (9) Enomoto, T.; Ohmoto, M.; Iwata, T.; Uno, A.; Saitou, M.; Yamaguchi, T.; Kominami, R.; Matsumoto, I.; Hirota, J. *Bcl11b/Ctip2* Controls the Differentiation of Vomeronasal Sensory Neurons in Mice. *J. Neurosci.* **2011**, *31*, 10159–10173.
- (10) Albu, D. I.; Feng, D.; Bhattacharya, D.; Jenkins, N. A.; Copeland, N. G.; Liu, P.; Avram, D. BCL11B is required for positive selection and survival of double-positive thymocytes. *J. Exp. Med.* **2007**, *204*, 3003–3015.
- (11) Li, P.; Burke, S.; Wang, J.; Chen, X.; Ortiz, M.; Lee, S.-C.; Lu, D.; Campos, L.; Goulding, D.; Ng, B. L.; et al. Reprogramming of T Cells to Natural Killer-Like Cells upon *Bcl11b* Deletion. *Science* **2010**, *329*, 85–89.
- (12) Li, L.; Leid, M.; Rothenberg, E. V. An Early T Cell Lineage Commitment Checkpoint Dependent on the Transcription Factor *Bcl11b*. *Science* **2010**, *329*, 89–93.
- (13) Leid, M.; Ishmael, J. E.; Avram, D.; Shepherd, D.; Fraulob, V.; Dollé, P. CTIP1 and CTIP2 are differentially expressed during mouse embryogenesis. *Gene Expr. Patterns* **2004**, *4*, 733–739.
- (14) Kastner, P.; Chan, S.; Vogel, W. K.; Zhang, L.-J.; Topark-Ngarm, A.; Golonzhka, O.; Jost, B.; Le Gras, S.; Gross, M. K.; Leid, M. *Bcl11b* represses a mature T-cell gene expression program in immature CD4<sup>+</sup>CD8<sup>+</sup> thymocytes. *Eur. J. Immunol.* **2010**, *40*, 2143–2154.
- (15) Ikawa, T.; Hirose, S.; Masuda, K.; Kakugawa, K.; Satoh, R.; Shibano-Satoh, A.; Kominami, R.; Katsura, Y.; Kawamoto, H. An Essential Developmental Checkpoint for Production of the T Cell Lineage. *Science* **2010**, *329*, 93–96.
- (16) Bernard, O. A.; Busson-LeConiat, M.; Ballerini, P.; Mauchauffé, M.; Valle, Della, V.; Monni, R.; Nguyen Khac, F.; Mercher, T.; Penard-Lacronique, V.; Pasturaud, P.; et al. A new recurrent and

specific cryptic translocation, t(5;14)(q35;q32), is associated with expression of the Hox11L2 gene in T acute lymphoblastic leukemia. *Leukemia* **2001**, *15*, 1495–1504.

(17) Berger, R.; Dastugue, N.; Busson, M.; Van Den Akker, J.; Pérot, C.; Ballerini, P.; Hagemeyer, A.; Michaux, L.; Charrin, C.; Pages, M. P.; et al. t(5;14)/HOX11L2-positive T-cell acute lymphoblastic leukemia. A collaborative study of the Groupe Français de Cytogénétique Hématologique (GFCH). *Leukemia* **2003**, *17*, 1851–1857.

(18) MacLeod, R. A. F.; Nagel, S.; Kaufmann, M.; Janssen, J. W. G.; Drexler, H. G. Activation of *HOX11L2* by Juxtaposition With 3'-*BCL11B* in an Acute Lymphoblastic Leukemia Cell Line (HPB-ALL) With t(5;14)(q35;q32.2). *Genes Chromosomes Cancer* **2003**, *37*, 84–91.

(19) Kurosawa, N.; Fujimoto, R.; Ozawa, T.; Itoyama, T.; Sadamori, N.; Isobe, M. Reduced Level of the BCL11B Protein Is Associated with Adult T-Cell Leukemia/Lymphoma. *PLoS ONE* **2013**, *8*, e55147.

(20) Abbas, S.; Sanders, M.; Zeilemaker, A.; Geertsma-Kleinekoort, W. M. C.; Koenders, J. E.; Kavelaars, F. G.; Abbas, Z. G.; Mahamoud, S.; Chu, I. W. T.; Hoogenboezem, R.; et al. Integrated genome-wide genotyping and gene expression profiling reveals BCL11B as a putative oncogene in acute myeloid leukemia with 14q32 aberrations. *Haematologica* **2014**.

(21) Ganguli-Indra, G.; Wasylyk, C.; Liang, X.; Millon, R.; Leid, M.; Wasylyk, B.; Abecassis, J.; Indra, A. K.; Indra, A. CTIP2 Expression in Human Head and Neck Squamous Cell Carcinoma is Linked to Poorly Differentiated Tumor Status. *PLoS ONE* **2009**, *4*, e5367.

(22) Kamimura, K.; Ohi, H.; Kubota, T.; Okazuka, K.; Yoshikai, Y.; Wakabayashi, Y.-I.; Aoyagi, Y.; Mishima, Y.; Kominami, R. Haploinsufficiency of *Bcl11b* for suppression of lymphomagenesis and thymocyte development. *Biochem Biophys Res Commun* **2007**, *355*, 538–542.

(23) Hornbeck, P. V.; Kornhauser, J. M.; Tkachev, S.; Zhang, B.; Skrzypek, E.; Murray, B.; Latham, V.; Sullivan, M. PhosphoSitePlus: a comprehensive resource for investigating the structure and function of experimentally determined post-translational modifications in man and mouse. *Nucl. Acids Res.* **2012**, *40*, D261–D270.

(24) Zhang, L.-J.; Vogel, W. K.; Liu, X.; Topark-Ngarm, A.; Arbogast, B. L.; Maier, C. S.; Filtz, T. M.; Leid, M. Coordinated Regulation of Transcription Factor Bcl11b Activity in Thymocytes by the Mitogen-activated Protein Kinase (MAPK) Pathways and Protein Sumoylation. *J. Biol. Chem.* **2012**, *287*, 26971–26988.

(25) Ohoka, Y.; Kuwata, T.; Tozawa, Y.; Zhao, Y.; Mukai, M.; Motegi, Y.; Suzuki, R.; Yokoyama, M.; Iwata, M. *In vitro* differentiation and commitment of CD4<sup>+</sup> CD8<sup>+</sup> thymocytes to the CD4 lineage, without TCR engagement. *Int. Immunol.* **1996**, *8*, 297–306.

(26) Takahama, Y.; Nakauchi, H. Phorbol Ester and Calcium Ionophore Can Replace TCR Signals That Induce Positive Selection of CD4 T Cells. *J. Immunol.* **1996**, *157*, 1508–1513.

(27) Frewen, B. E.; Merrihew, G. E.; Wu, C. C.; Noble, W. S.; MacCoss, M. J. Analysis of Peptide MS/MS Spectra from Large-Scale Proteomics Experiments Using Spectrum Libraries. *Anal. Chem.* **2006**, *78*, 5678–5684.

- (28) Maclean, B.; Tomazela, D. M.; Abbatiello, S. E.; Zhang, S.; Whiteaker, J. R.; Paulovich, A. G.; Carr, S. A.; MacCoss, M. J. Effect of Collision Energy Optimization on the Measurement of Peptides by Selected Reaction Monitoring (SRM) Mass Spectrometry. *Anal. Chem.* **2010**, *82*, 10116–10124.
- (29) Maclean, B.; Tomazela, D. M.; Shulman, N.; Chambers, M.; Finney, G. L.; Frewen, B.; Kern, R.; Tabb, D. L.; Liebler, D. C.; MacCoss, M. J. Skyline: an open source document editor for creating and analyzing targeted proteomics experiments. *Bioinformatics* **2010**, *26*, 966–968.
- (30) Gross, E.; Witkop, B. Nonenzymatic Cleavage of Peptide Bonds: The Methionine Residues in Bovine Pancreatic Ribonuclease. *J. Biol. Chem.* **1962**, *237*, 1856–1860.
- (31) Farrah, T.; Deutsch, E. W.; Kreisberg, R.; Sun, Z.; Campbell, D. S.; Mendoza, L.; Kusebauch, U.; Brusniak, M.-Y.; Hüttenhain, R.; Schiess, R.; et al. PASSEL: The PeptideAtlas SRMexperiment library. *Proteomics* **2012**, *12*, 1170–1175.
- (32) Ni, W.; Xu, S.-L.; Chalkley, R. J.; Pham, T. N. D.; Guan, S.; Maltby, D. A.; Burlingame, A. L.; Wang, Z.-Y.; Quail, P. H. Multisite Light-Induced Phosphorylation of the Transcription Factor PIF3 Is Necessary for Both Its Rapid Degradation and Concomitant Negative Feedback Modulation of Photoreceptor phyB Levels in *Arabidopsis*. *Plant Cell* **2013**, *25*, 2679–2698.
- (33) Zheng, H.; Seit-Nebi, A.; Han, X.; Aslanian, A.; Tat, J.; Liao, R.; Yates, J. R.; Sun, P. A posttranslational modification cascade involving p38, Tip60, and PRAK mediates oncogene-induced senescence. *Mol. Cell* **2013**, *50*, 699–710.
- (34) Mayya, V.; Lundgren, D. H.; Hwang, S.-I.; Rezaul, K.; Wu, L.; Eng, J. K.; Rodionov, V.; Han, D. K. Quantitative Phosphoproteomic Analysis of T Cell Receptor Signaling Reveals System-Wide Modulation of Protein-Protein Interactions. *Sci. Signal.* **2009**, *2*, ra46.

- (35) Gerber, S. A.; Rush, J.; Stemman, O.; Kirschner, M. W.; Gygi, S. P. Absolute quantification of proteins and phosphoproteins from cell lysates by tandem MS. *Proc. Natl. Acad. Sci. U. S. A.* **2003**, *100*, 6940–6945.
- (36) Kirkpatrick, D. S.; Gerber, S. A.; Gygi, S. P. The absolute quantification strategy: a general procedure for the quantification of proteins and post-translational modifications. *Methods* **2005**, *35*, 265–273.
- (37) Ulrich, H. D. The Fast-Growing Business of SUMO Chains. *Mol. Cell* **2008**, *32*, 301–305.
- (38) Rohr, O.; Lecestre, D.; Chasserot-Golaz, S.; Marban, C.; Avram, D.; Aunis, D.; Leid, M.; Schaeffer, E. Recruitment of Tat to Heterochromatin Protein HP1 via Interaction with CTIP2 Inhibits Human Immunodeficiency Virus Type 1 Replication in Microglial Cells. *J. Virol.* **2003**, *77*, 5415–5427.
- (39) Senawong, T.; Peterson, V. J.; Avram, D.; Shepherd, D. M.; Frye, R. A.; Minucci, S.; Leid, M. Involvement of the Histone Deacetylase SIRT1 in Chicken Ovalbumin Upstream Promoter Transcription Factor (COUP-TF)-interacting Protein 2-mediated Transcriptional Repression. *J. Biol. Chem.* **2003**, *278*, 43041–43050.
- (40) Marban, C.; Redel, L.; Suzanne, S.; Van Lint, C.; Lecestre, D.; Chasserot-Golaz, S.; Leid, M.; Aunis, D.; Schaeffer, E.; Rohr, O. COUP-TF interacting protein 2 represses the initial phase of HIV-1 gene transcription in human microglial cells. *Nucl. Acids Res.* **2005**, *33*, 2318–2331.
- (41) Topark-Ngarm, A.; Golonzhka, O.; Peterson, V. J.; Barrett, B.; Martinez, B.; Crofoot, K.; Filtz, T. M.; Leid, M. CTIP2 Associates with the NuRD Complex on the Promoter of *p57KIP2*, a Newly Identified CTIP2 Target Gene. *J. Biol. Chem.* **2006**, *281*, 32272–32283.

(42) Farrell, A. S.; Pelz, C.; Wang, X.; Daniel, C. J.; Wang, Z.; Su, Y.; Janghorban, M.; Zhang, X.; Morgan, C.; Impey, S.; et al. Pin1 regulates the dynamics of c-Myc DNA binding to facilitate target gene regulation and oncogenesis. *Mol. Cell. Biol.* **2013**, *33*, 2930–2949.

(43) Mendoza, M. C.; Er, E. E.; Zhang, W.; Ballif, B. A.; Elliott, H. L.; Danuser, G.; Blenis, J. ERK-MAPK Drives Lamellipodia Protrusion by Activating the WAVE2 Regulatory Complex. *Mol. Cell* **2011**, *41*, 661–671.

(44) Mendoza, H.; Campbell, D. G.; Burness, K.; Hastie, J.; Ronkina, N.; Shim, J.-H.; Arthur, J. S. C.; Davis, R. J.; Gaestel, M.; Johnson, G. L.; et al. Roles for TAB1 in regulating the IL-1-dependent phosphorylation of the TAB3 regulatory subunit and activity of the TAK1 complex. *Biochem. J.* **2008**, *409*, 711–722.

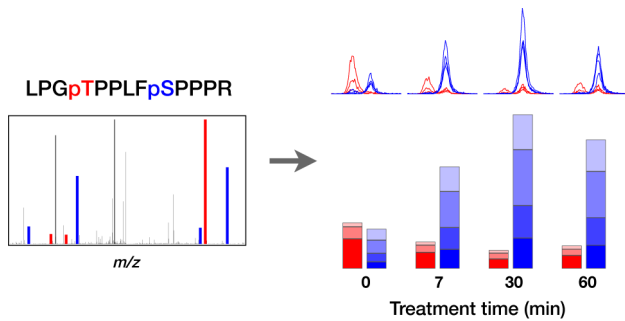
(45) Okamura, H.; Aramburu, J.; García-Rodríguez, C.; Viola, J. P.; Raghavan, A.; Tahiliani, M.; Zhang, X.; Qin, J.; Hogan, P. G.; Rao, A. Concerted dephosphorylation of the transcription factor NFAT1 induces a conformational switch that regulates transcriptional activity. *Mol. Cell* **2000**, *6*, 539–550.

(46) Salazar, C.; Brümmer, A.; Alberghina, L.; Höfer, T. Timing control in regulatory networks by multisite protein modifications. *Trends Cell Biol.* **2010**, *20*, 634–641.

(47) Kõivomägi, M.; Valk, E.; Venta, R.; Iofik, A.; Lepiku, M.; Balog, E. R. M.; Rubin, S. M.; Morgan, D. O.; Loog, M. Cascades of multisite phosphorylation control Sic1 destruction at the onset of S phase. *Nature* **2011**, *480*, 128–131.

(48) Niewiadomski, P.; Kong, J. H.; Ahrends, R.; Ma, Y.; Humke, E. W.; Khan, S.; Teruel, M. N.; Novitch, B. G.; Rohatgi, R. Gli Protein Activity Is Controlled by Multisite Phosphorylation in Vertebrate Hedgehog Signaling. *Cell Rep.* **2014**, *6*, 168–181.

For Table of Contents Only



## Supporting Information

***SUPPLEMENTAL FIGURE 1***

Outline of BCL11B sample preparation

***SUPPLEMENTAL FIGURE 2***

BCL11B sample preparation: gel purification

***SUPPLEMENTAL FIGURE 3***

Spectra database matches for analyzed peptides

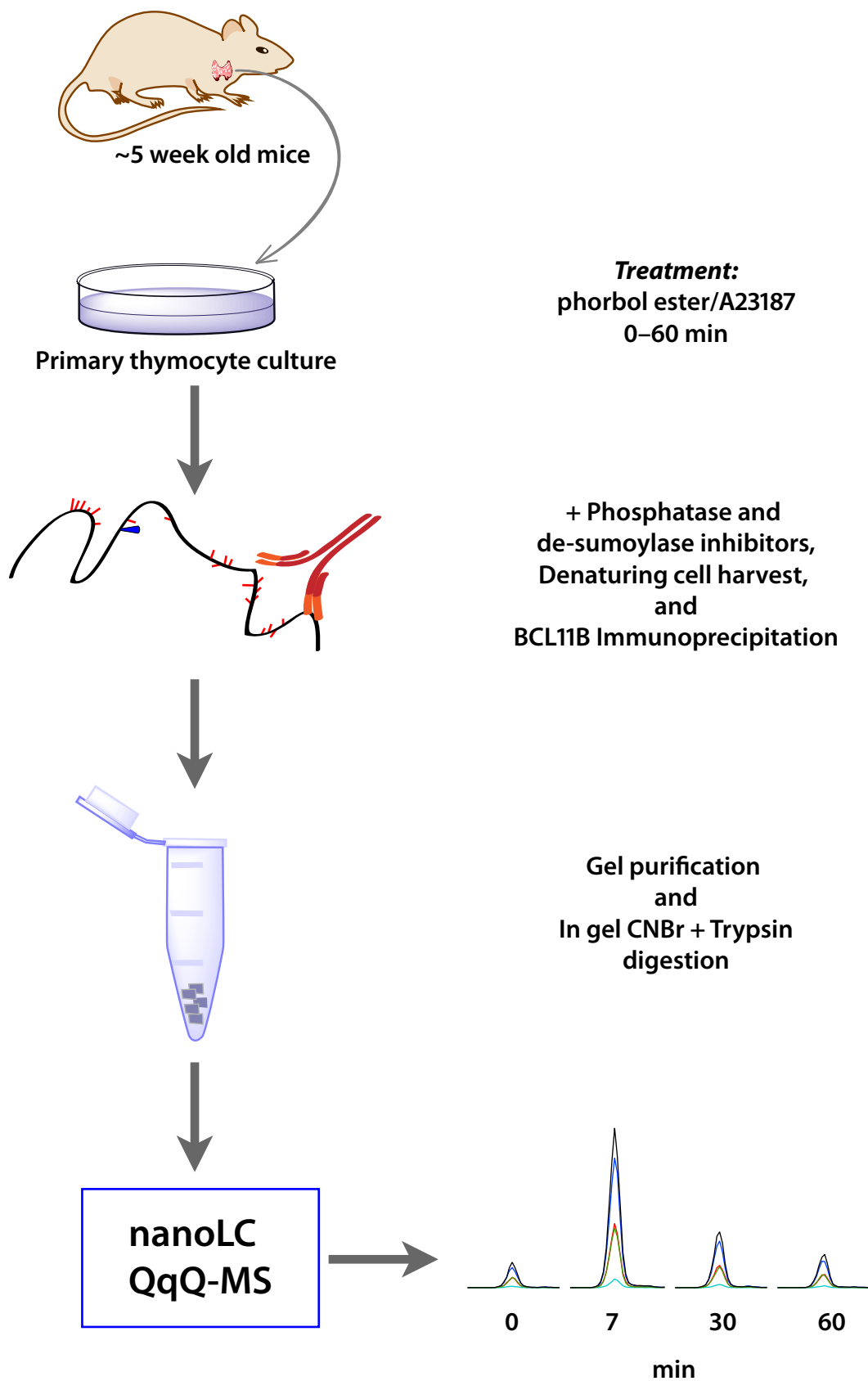
***SUPPLEMENTAL FIGURE 4***

Relative quantification of BCL11B peptides used to normalize PTM-containing peptide signals

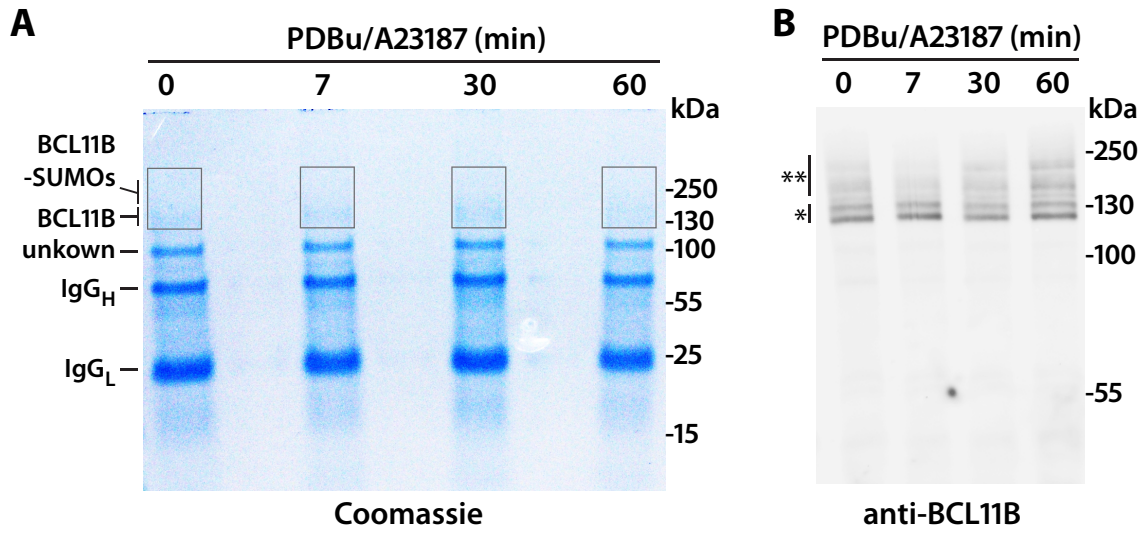
***SUPPLEMENTAL FIGURE 5***

Quantitative immunoblot analysis of BCL11B sumoylation

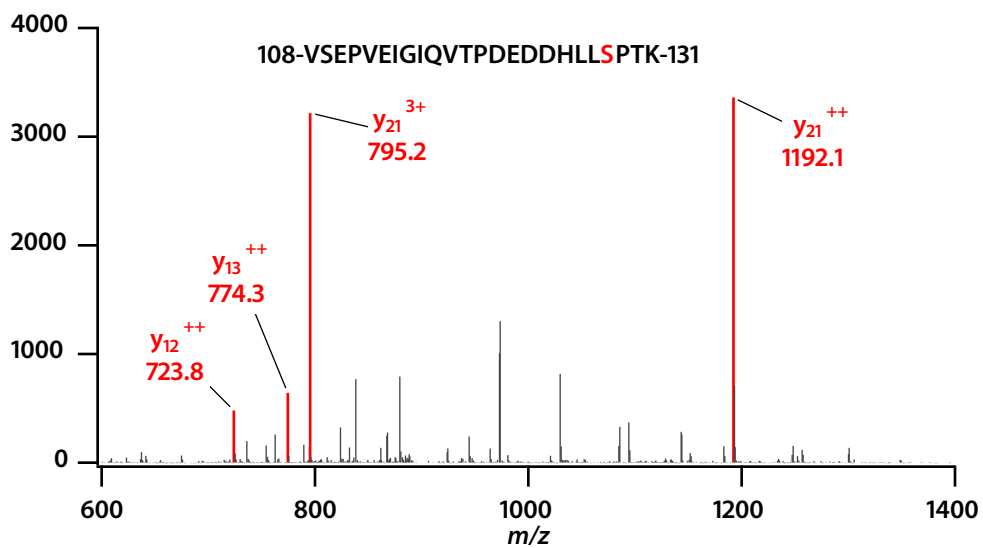
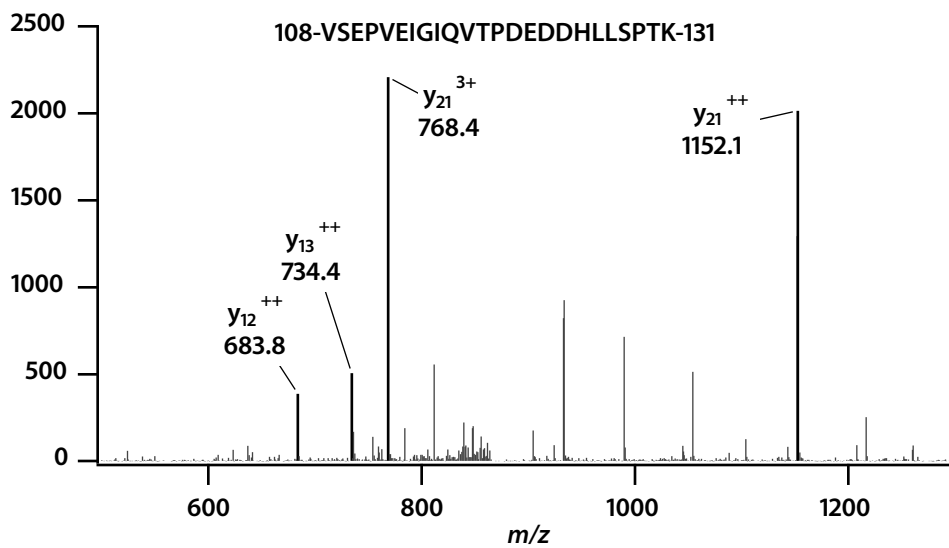
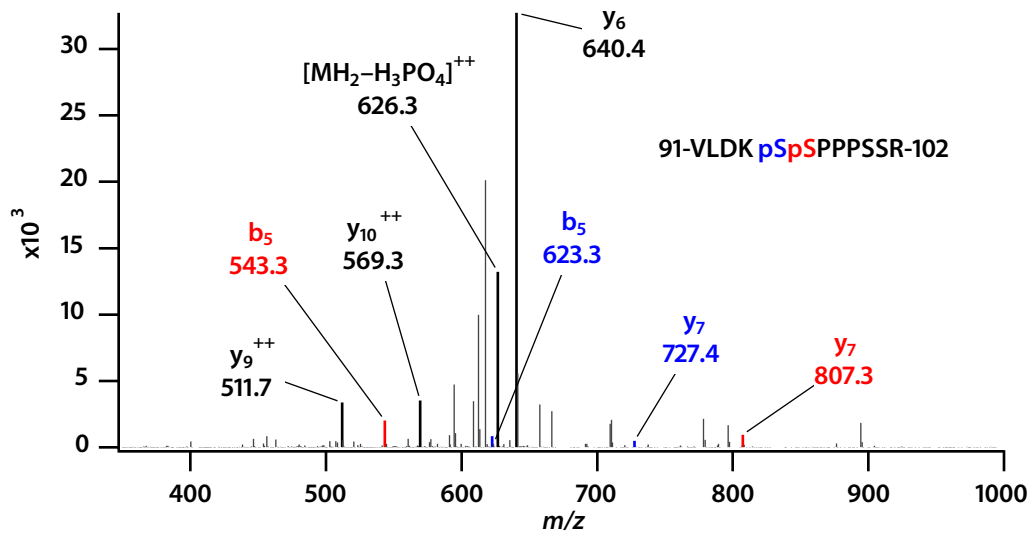


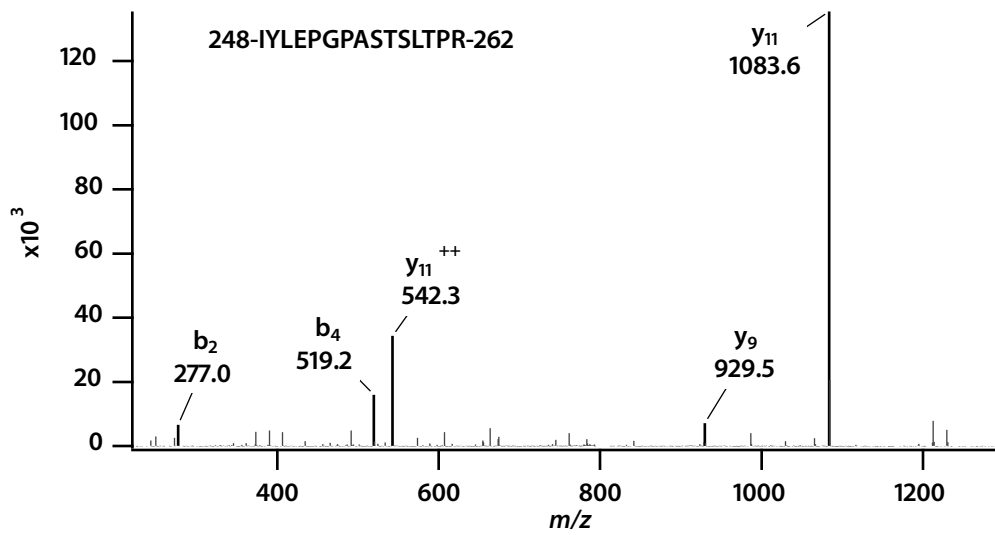
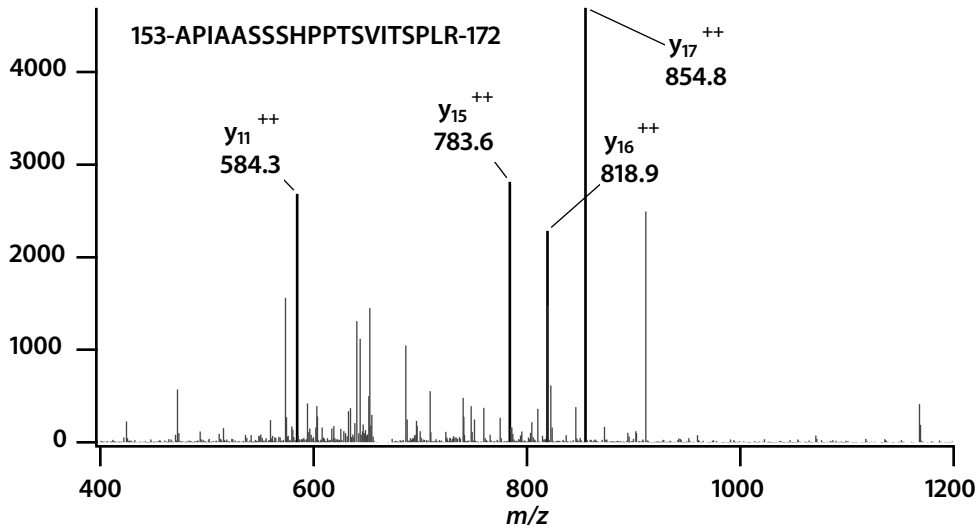
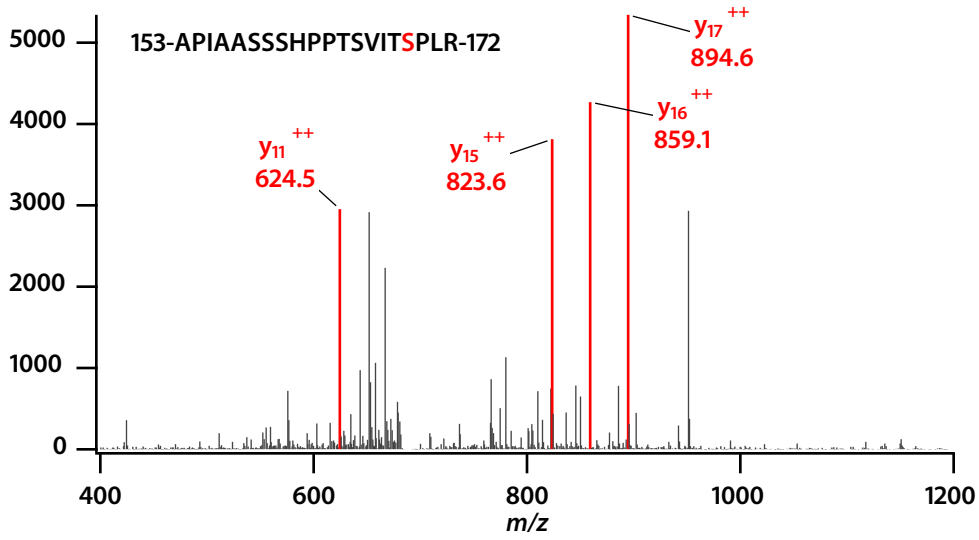


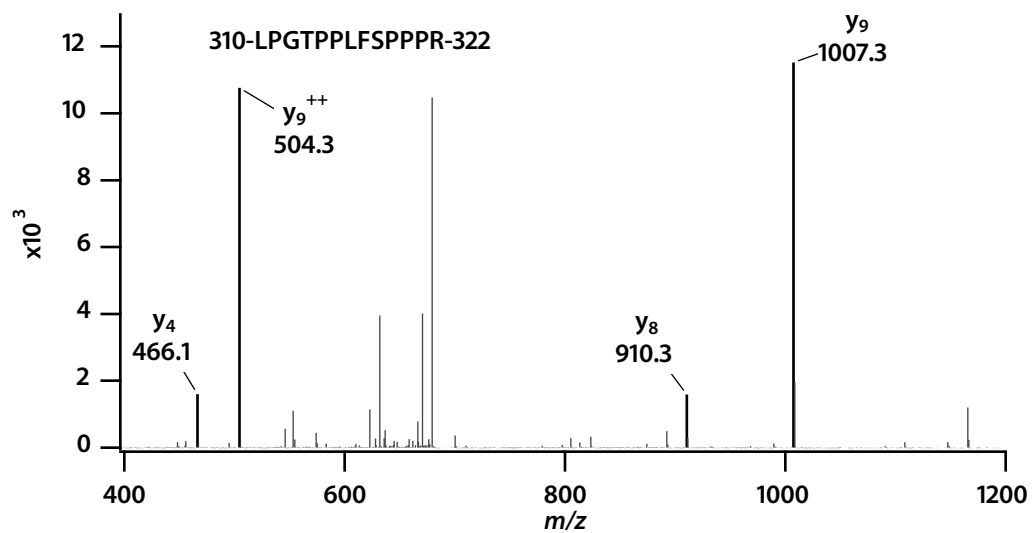
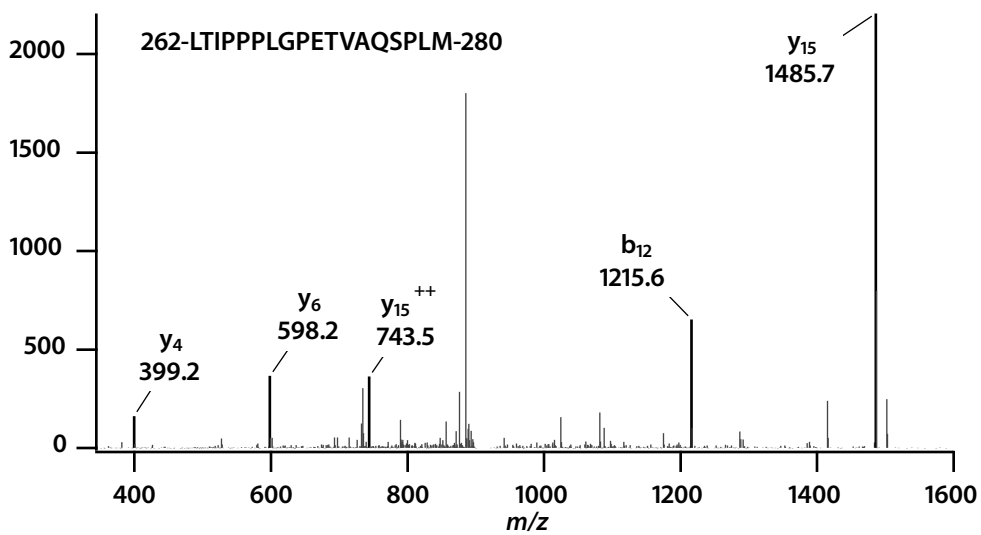
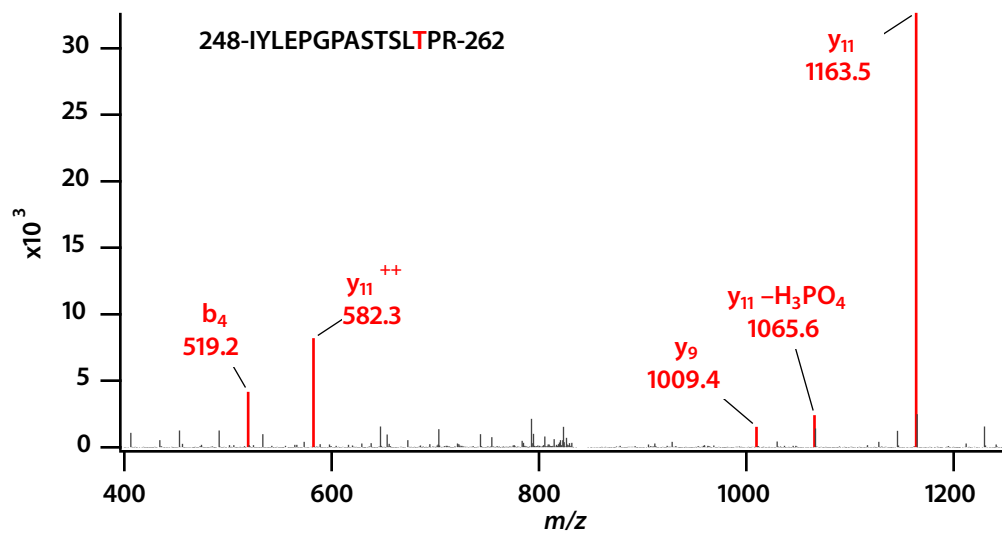
SUPPLEMENTAL FIGURE 1. Outline of BCL11B sample preparation.

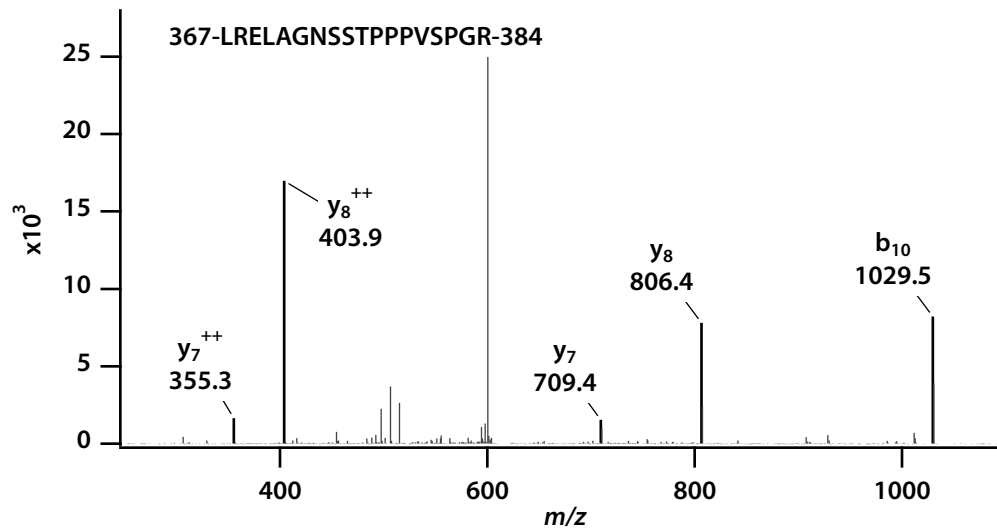
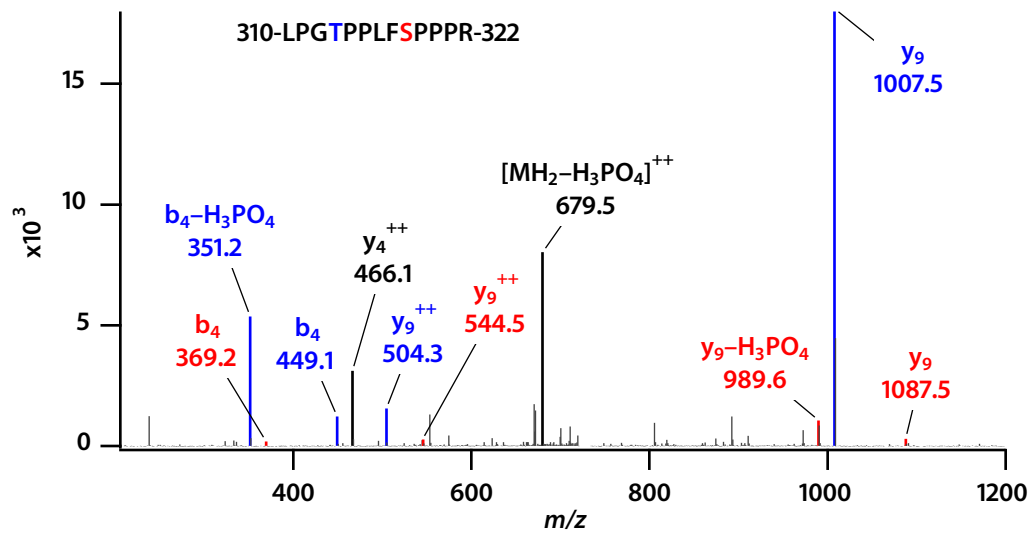
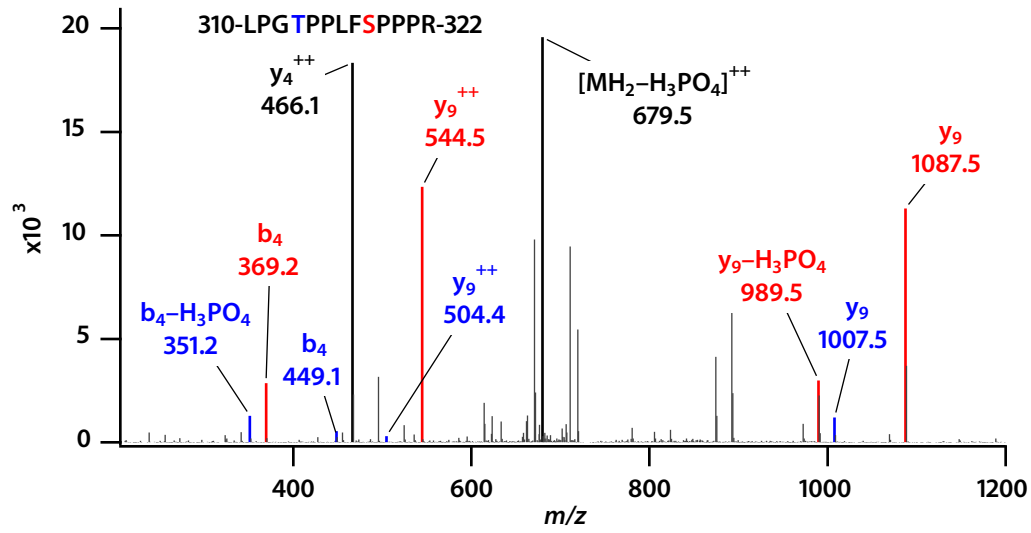


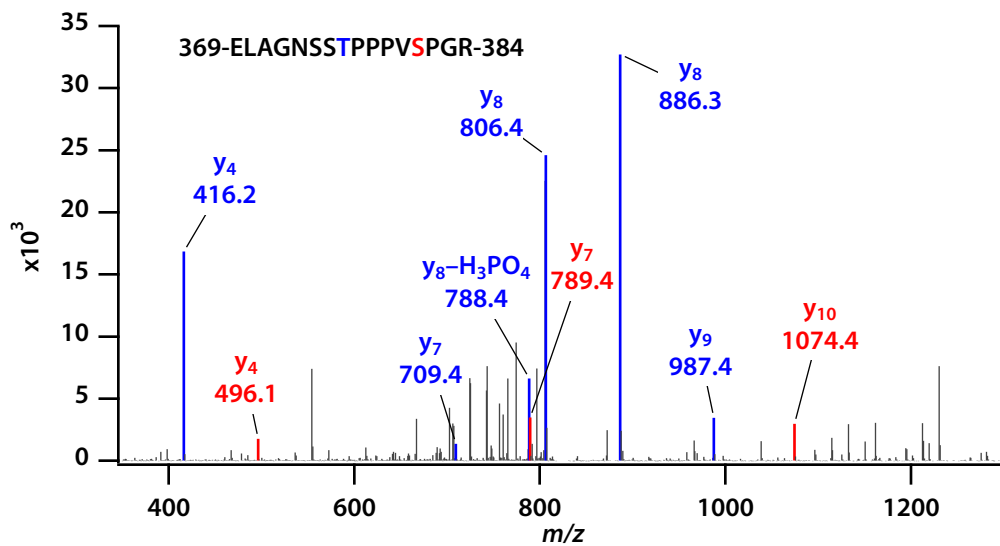
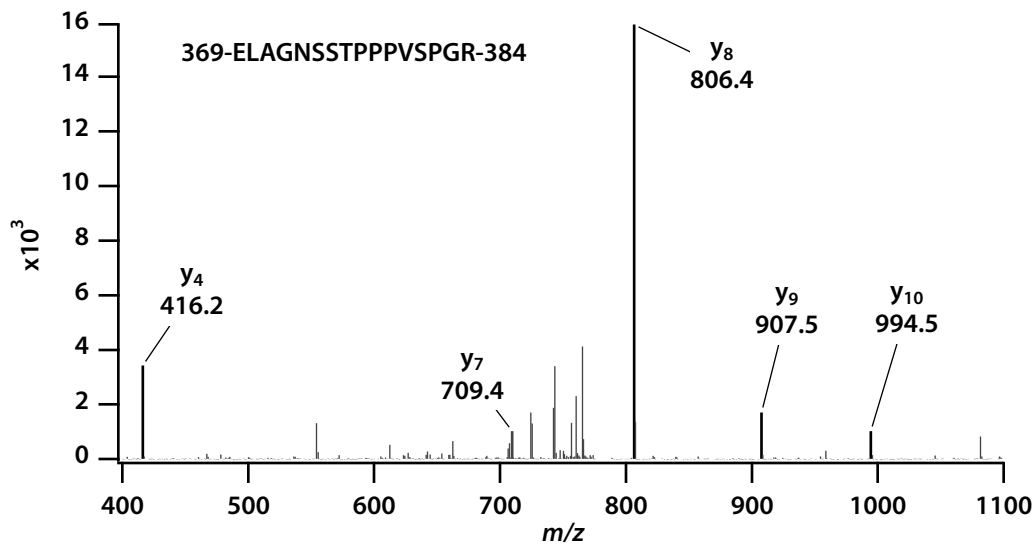
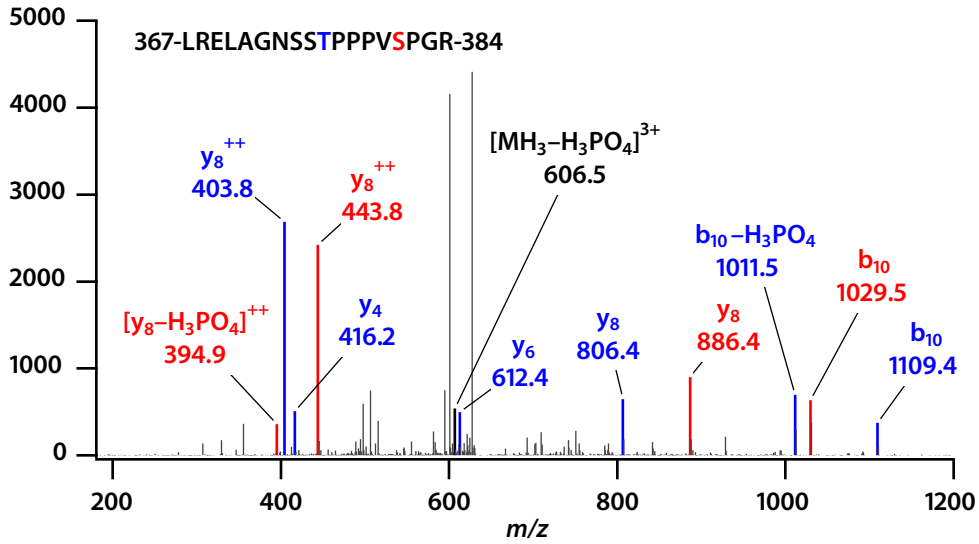
SUPPLEMENTAL FIGURE 2. **BCL11B sample preparation: gel purification.** Analytical samples containing both BCL11B and SUMO-modified BCL11B isoforms were prepared from denatured cell extracts immunoprecipitated with anti-BCL11B. **A.** Electrophoretically-purified BCL11B samples encompassing both unsumoylated and sumoylated forms were excised from Coomassie Blue G250 stained PAGE gels and cleaved into peptides by sequential cyanogen bromide chemical cleavage and trypsin digestion. The figure shows a qualification gel used in these studies and the regions analyzed are outlined by gray boxes. The unsumoylated BCL11B doublet, full-length protein and a slice-isoform variant, were visible to the naked eye but photographed poorly. **B.** Anti-BCL11B immunoblot analysis of anti-BCL11B immunoprecipitated preparative extract is shown. The vertical bars in the figure identify the unsumoylated BCL11B doublet (\*) and the SUMO1 and SUMO2/3 modified forms (\*\*) previously identified.<sup>24</sup>

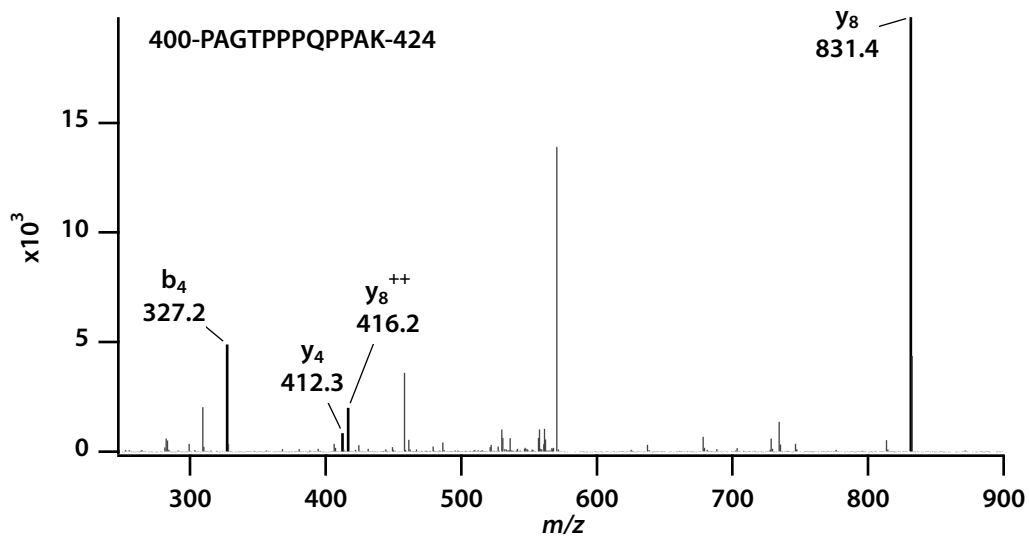
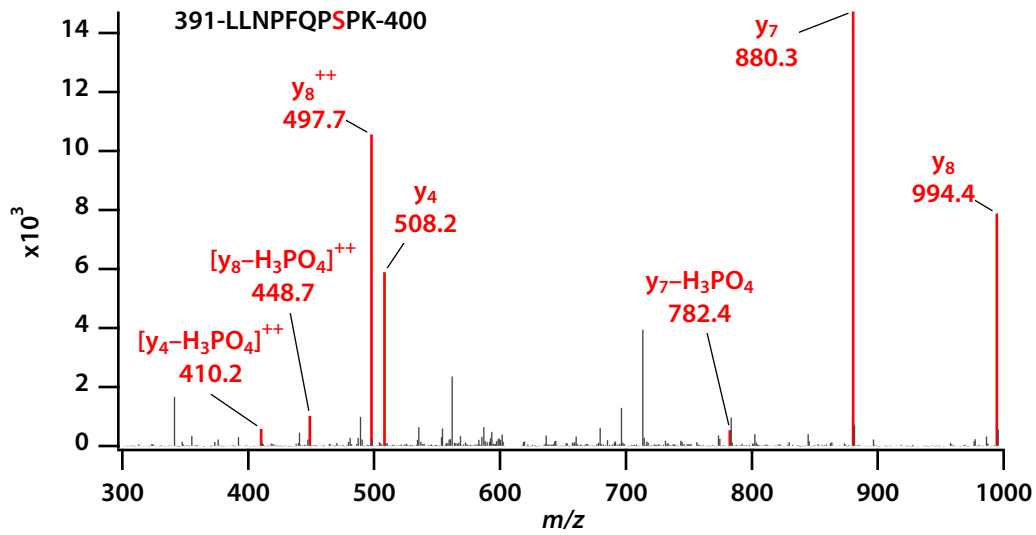
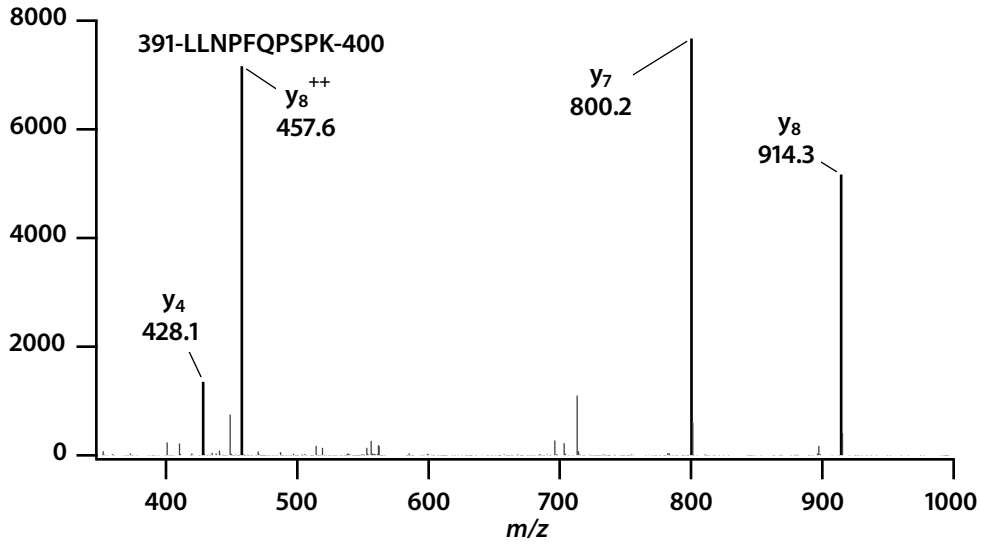




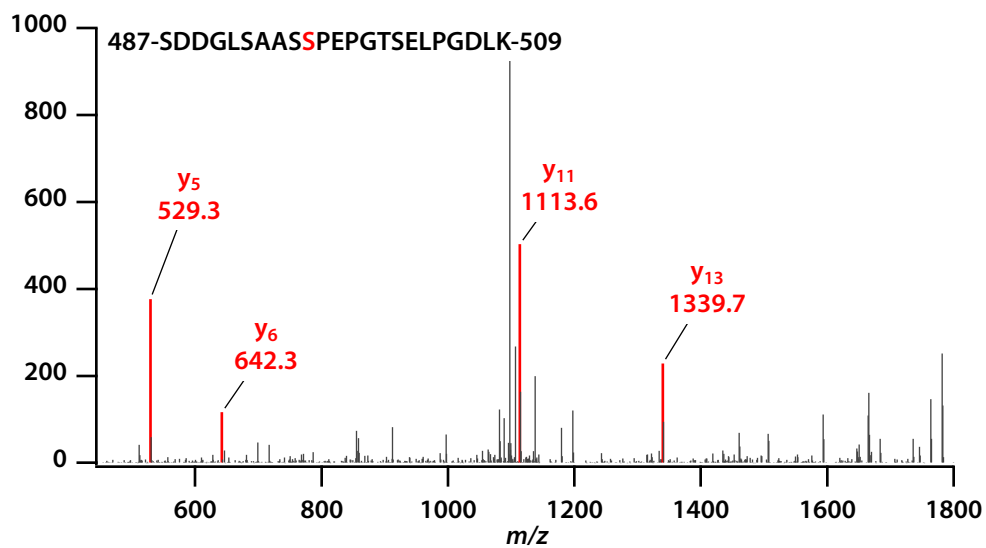
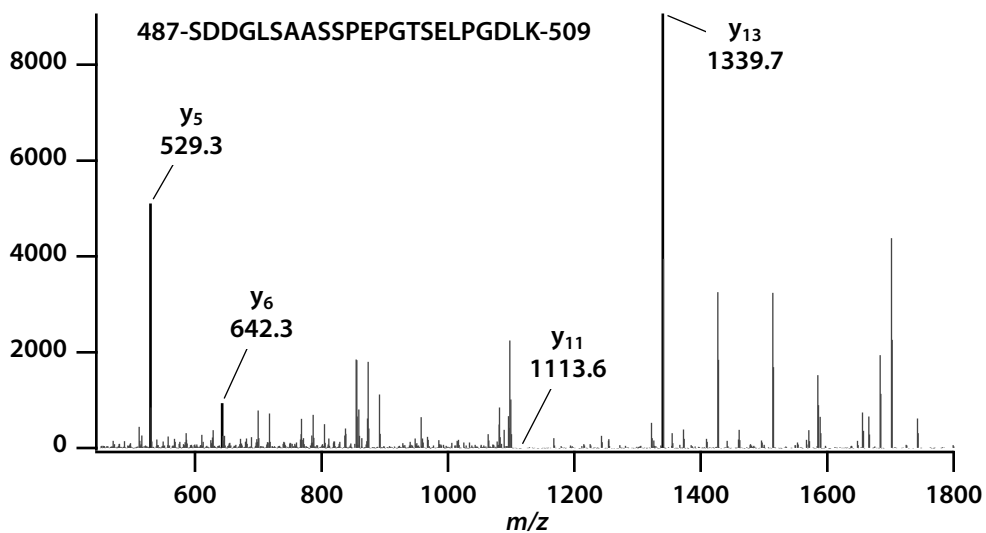
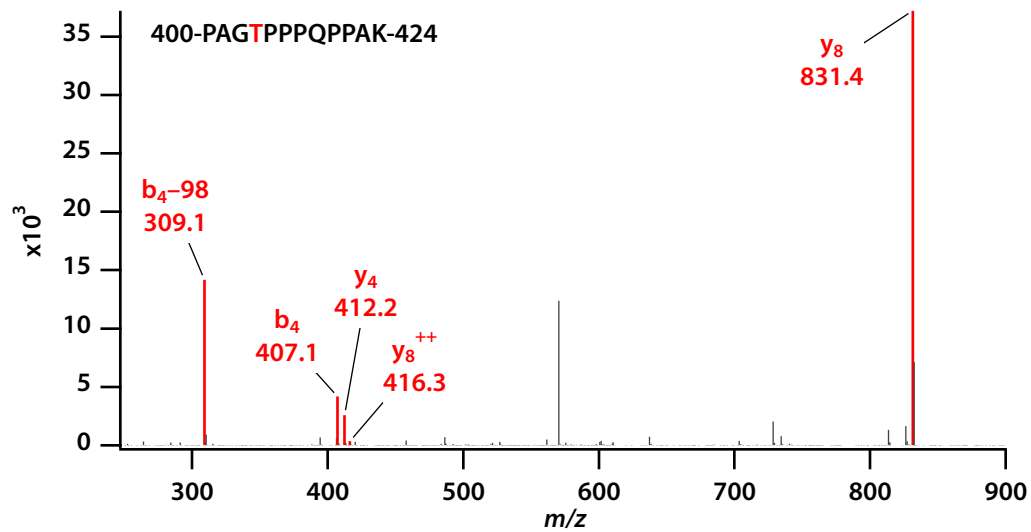


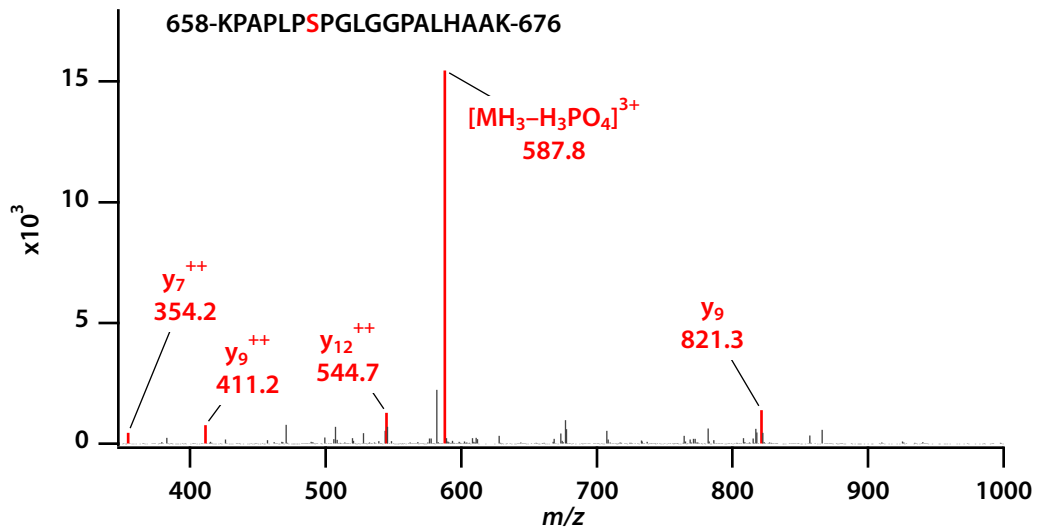
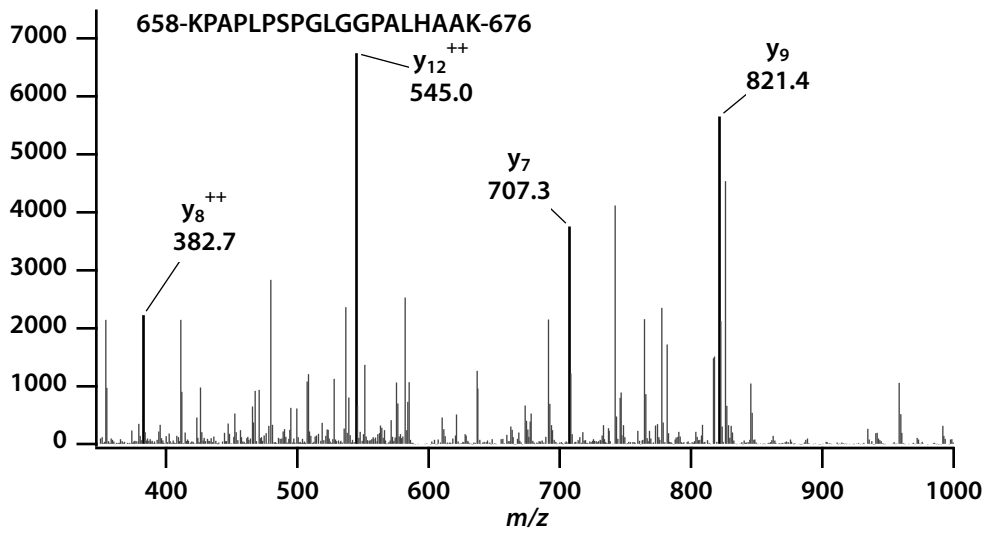
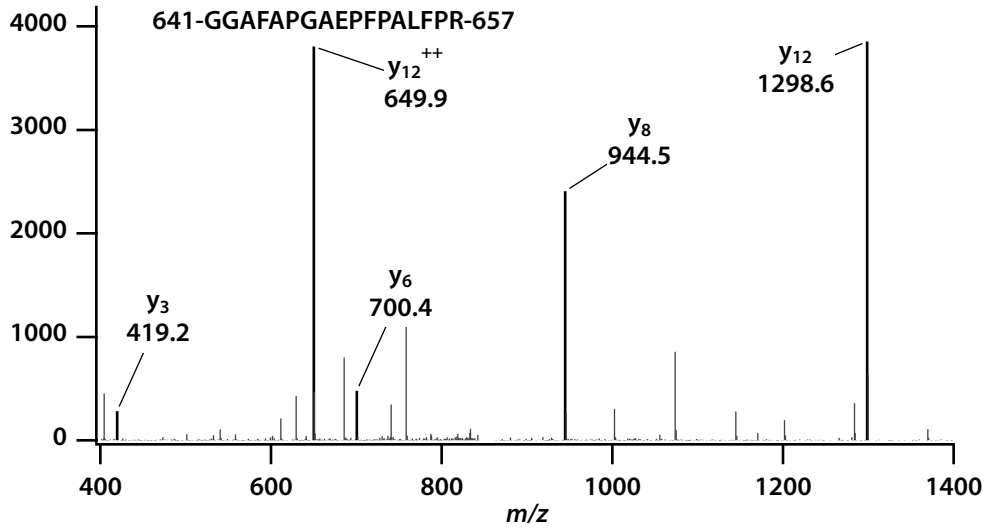


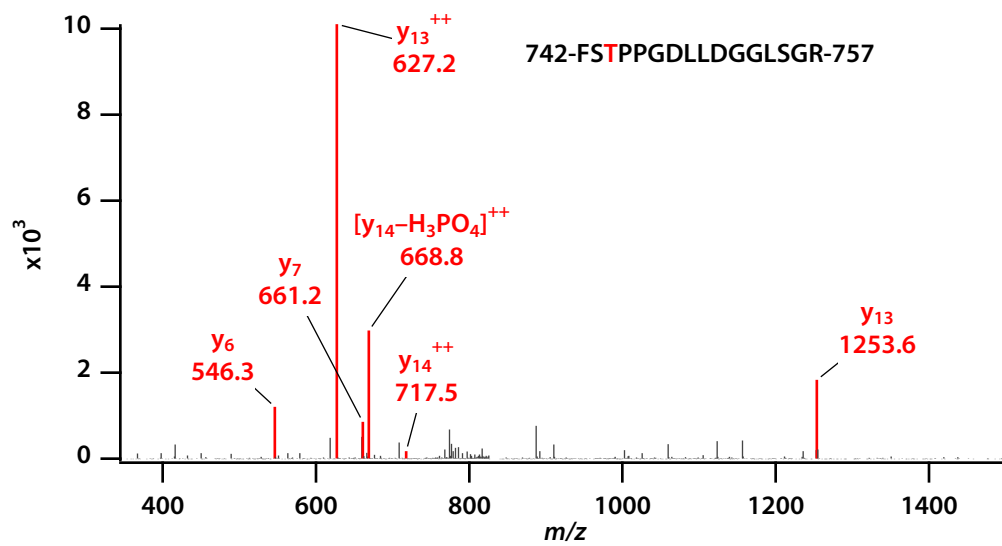
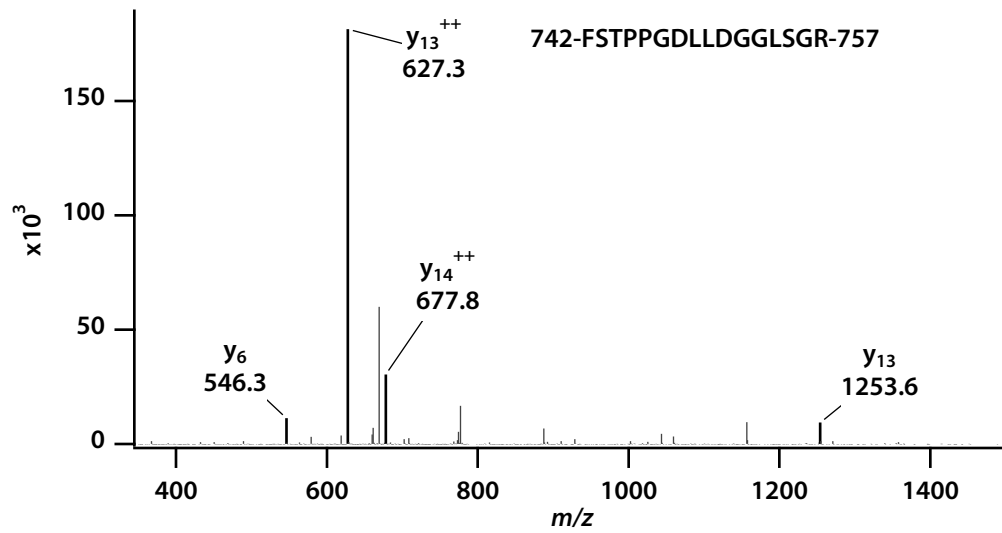
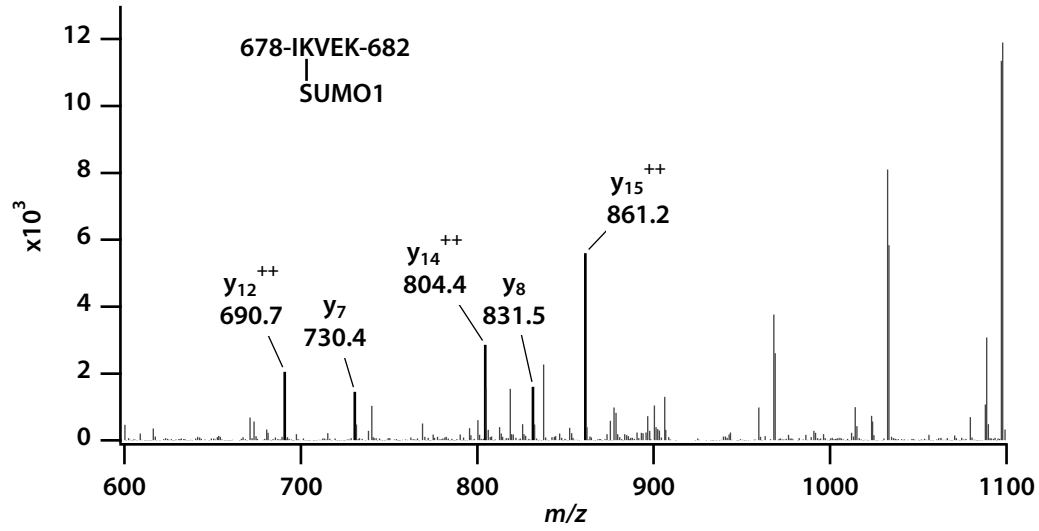


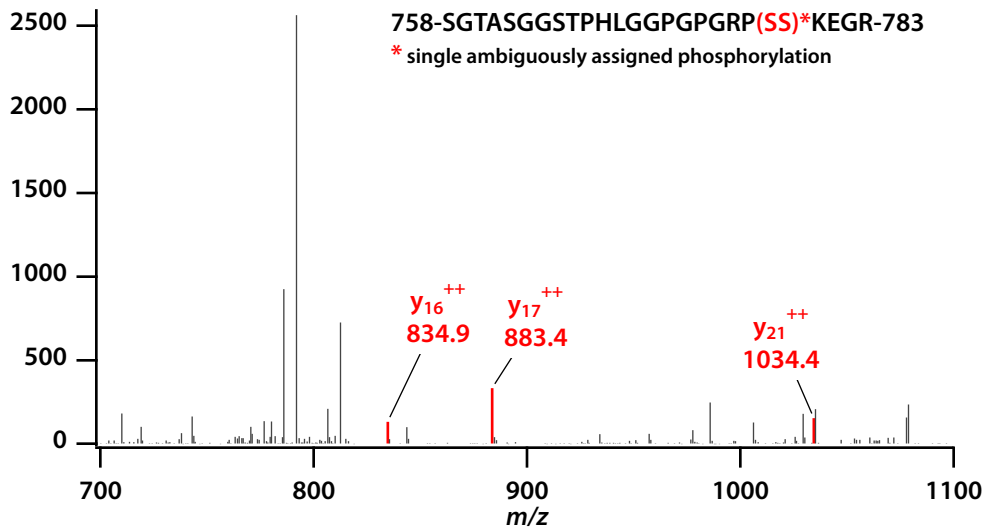
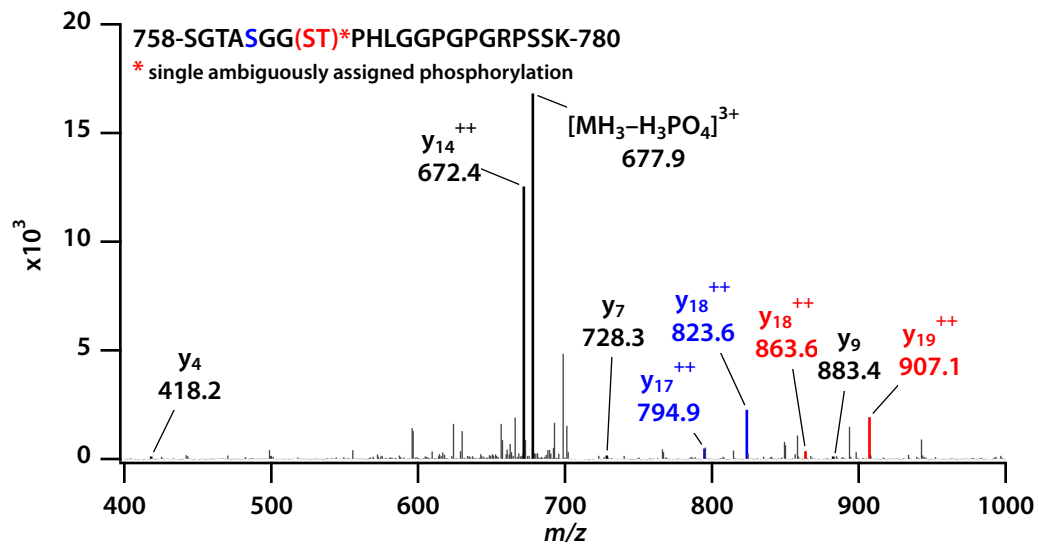
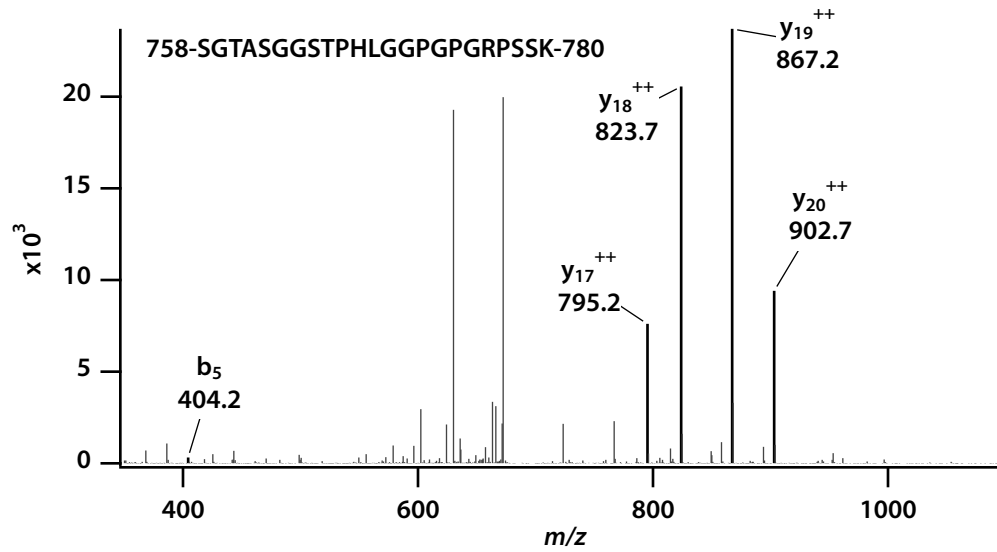




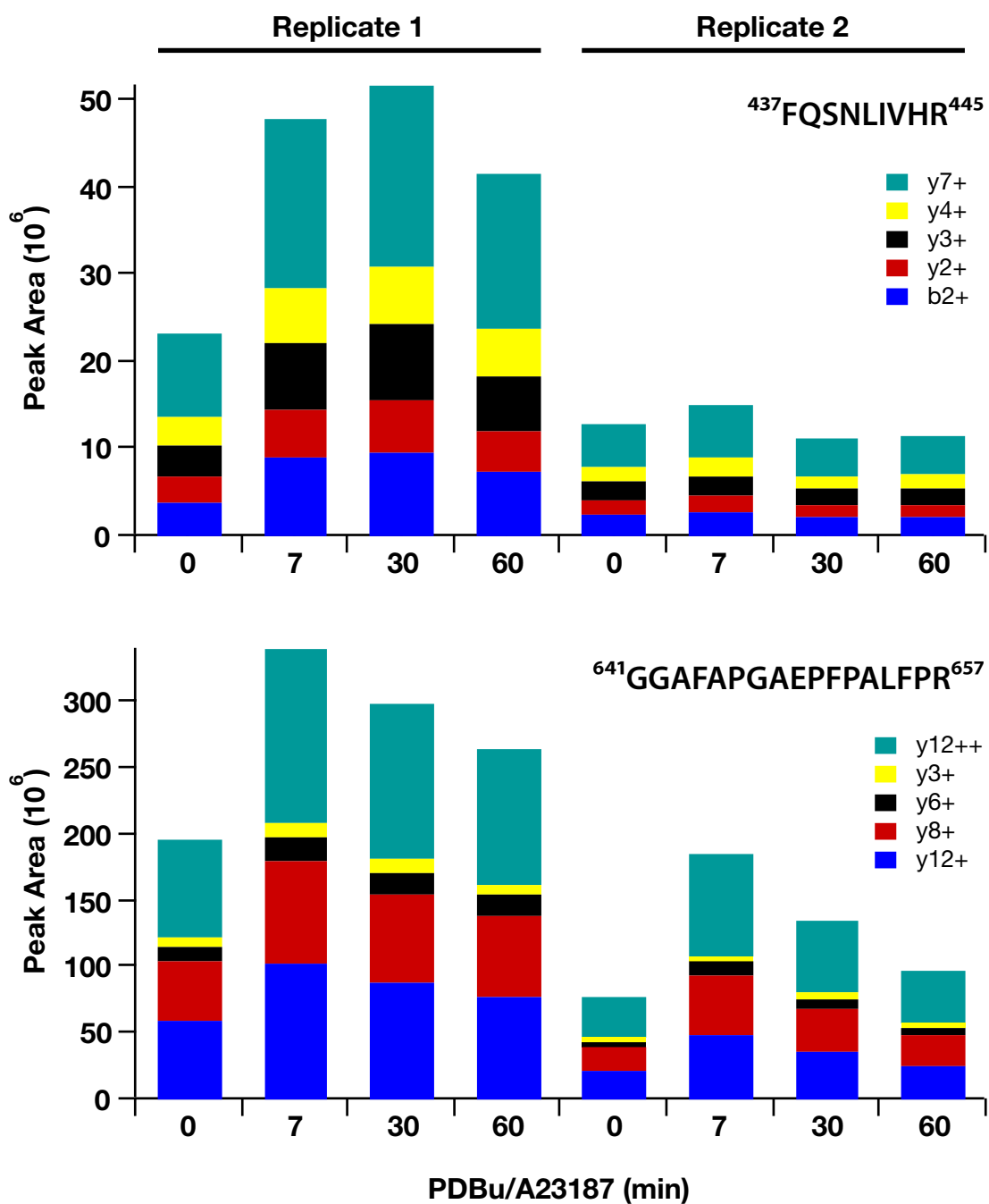




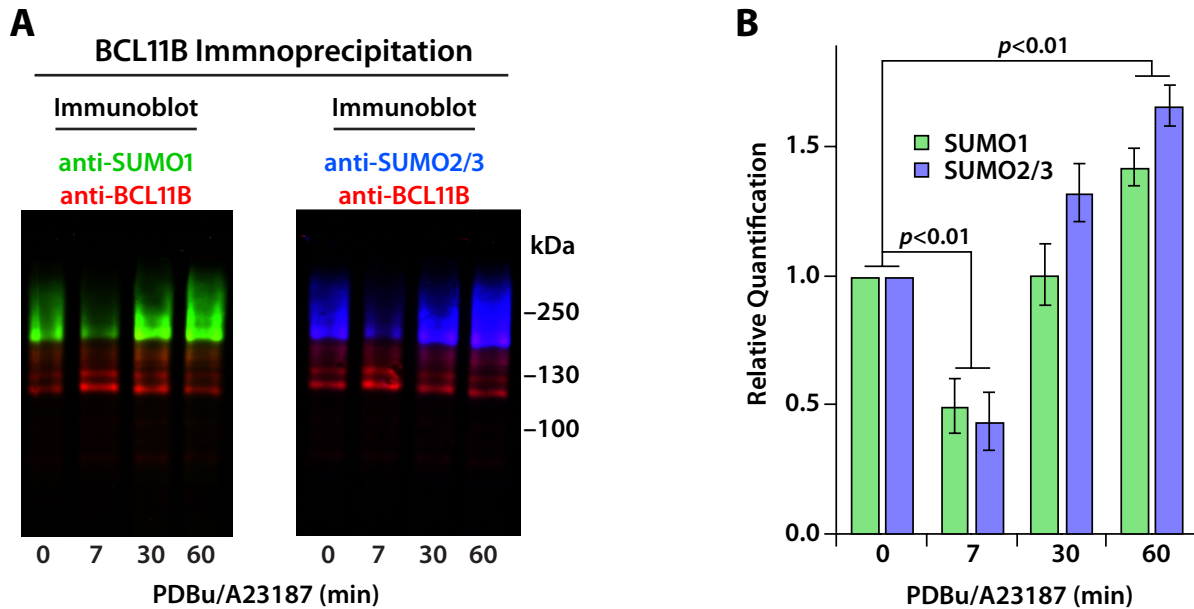




SUPPLEMENTAL FIGURE 3. **Spectra database matches for analyzed peptides.** Tandem mass spectra were recorded on an LTQ-FT mass spectrometer as described.<sup>24</sup> Analyzed transitions are shown labeled and phosphosite-specific transitions are colored red and/or blue to indicated the specific transitions used for phosphorylation site quantification.



SUPPLEMENTAL FIGURE 4. **Relative quantification of BCL11B peptides used to normalize PTM-containing peptide signals.** BCL11B peptides were quantified by multiple reaction monitoring on a nanoflow LC-coupled Thermo TSQ Vantage triple quadrupole mass spectrometer. Precursor/fragment ion pair currents were recorded and integrated peak areas for each are presented as a stacked histogram, the sum of which is the quantitative value. See Supplemental Table 1 for optimized collisional energies used during the collection of each ion pair. Results from both biological replicates are shown.



SUPPLEMENTAL FIGURE 5. **Quantitative immunoblot analysis of BCL11B sumoylation.** The covalent attachment of SUMO1 and SUMO2/3 moieties to BCL11B was examined in primary mouse thymocytes following cellular stimulation by phorbol ester and calcium ionophore. **A.** BCL11B was immunoprecipitated from denatured cell extracts as described in Materials and Methods, size resolved on SDS-PAGE gels (10% BisTris/MOPS), and transferred to nitrocellulose for immunoblot analysis. Immunoblot analyses used rat primary antibody to BCL11B (Abcam ab18465) in combination with either rabbit anti-SUMO1 (Abcam ab32058) or rabbit anti-SUMO2/3 (Abcam ab3742), followed by IRDye680LT-conjugated anti-rat and IRDye800CW-conjugated anti-rabbit secondary antibodies used in combination. Dual-channel fluorescence signal was recorded on an Odyssey near-infrared fluorescence imager (LI-COR Biosystems, Lincoln, NE). Immunofluorescence is shown in false color with BCL11B signal shown in red, SUMO1 signal in green, and SUMO2/3 signal in blue. **B.** Fluorescence-signal-quantified BCL11B sumoylation levels are shown relative to unstimulated control (time 0). SUMO1-BCL11B ratio values are plotted in green, SUMO2/3-BCL11B ratio values are plotted in blue, and error bars indicate the standard error of the mean from four biological replicate determinations ( $n = 4$ ). For both subtypes, relative sumoylation levels were less than basal (time 0) after 7 min of stimulation and greater than basal after 60 min, but not significantly different from basal after 30 min ( $p < 0.01$ ).